ASTROBIOLOGY
Volume 8, Number 1, 2008

DOI: 10.1089/ast.2007.0130

Research Paper

Subsurface Filamentous Fabrics: An Evaluation of Origins Based on Morphological and Geochemical Criteria, with Implications for Exopaleontology

BEDA A. HOFMANN,[1] JACK D. FARMER,[2] FRIEDHELM VON BLANCKENBURG,[3,*] and ANTHONY E. FALLICK[4]

ABSTRACT

The fossil record of the subsurface biosphere is sparse. Results obtained on subsurface filamentous fabrics (SFF) from >225 paleosubsurface sites in volcanics, oxidized ores, and paleokarst of subrecent to Proterozoic age are presented. SFF are mineral encrustations on filamentous or fibrous substrates that formed in subsurface environments. SFF occur in association with low-temperature aqueous mineral assemblages and consist of tubular, micron-thick (median 1.6 micron) filaments in high spatial density, which occur as irregular masses, matted fabrics, and vertically draped features that resemble stalactites. Micron-sized filamentous centers rule out a stalactitic origin. Morphometric analysis of SFF filamentous forms demonstrates that their shape more closely resembles microbial filaments than fibrous minerals. Abiogenic filament-like forms are considered unlikely precursors of most SFF, because abiogenic forms differ in the distribution of widths and have a lower degree of curvature and a lower number of direction changes. Elemental analyses of SFF show depletion in immobile elements (*e.g.*, Al, Th) and a systematic enrichment in As and Sb, which demonstrates a relation to environments with high flows of water. Sulfur isotopic analyses are consistent with a biological origin of a SFF sample from a Mississippi Valley–Type deposit, which is consistent with data in the literature. Fe isotopes in SFF and active analogue systems, however, allow no discrimination between biogenic and abiogenic origins. The origin of most SFF is explained as permineralized remains of microbial filaments that possibly record rapid growth during phases of high water flow that released chemical energy. It is possible that some SFF formed due to encrustation of mineral fibers. SFF share similarities with *Microcodium* from soil environments. SFF are a logical target in the search for past life on Mars. The macroscopic nature of many SFF allows for their relatively easy *in situ* recognition and targeting for more detailed microstructural and geochemical analysis. Key Words: Filaments—Subsurface—Microbes—Fossils—Morphology—Stable isotopes—Mars. Astrobiology 8, 87–117.

[1]Natural History Museum Bern, Bern, Switzerland.
[2]Department of Geological Sciences, Arizona State University, Tempe, Arizona.
[3]Institut für Geologie, University of Bern, Bern, Switzerland.
[4]Scottish Universities Environmental Research Centre, East Kilbride, Scotland.
[*]Present address: Institut für Mineralogie, Universität Hannover, Hannover, Germany.

INTRODUCTION

The discovery of a deep subsurface biosphere dominated by thermophilic, chemotrophic microbial life (Amy and Haldeman, 1997; D'Hondt *et al.*, 2004; Farmer, 2000; Ghiorse, 1997; Gold, 1992; Pedersen, 2000; Stevens, 1997; Stevens and McKinley, 1995) in continental and marine settings has revolutionized our thinking about the nature and environmental limits of microbial life on Earth and the potential for life elsewhere in the Solar System. While subsurface communities appear to be dominated by slowly growing chemotrophs (D'Hondt *et al.*, 2002), they may constitute half of Earth's biomass (Gold, 1999; Pedersen, 2000). Subsurface microbial life may also have played an important role in the early evolution of our biosphere. Life may have had its origin in deep subsurface environments, which could have been sheltered from the giant impacts that overlapped with the origin and early evolution of the biosphere.

Fossils are our only direct record of ancient life on Earth. Thus, proper evaluation of ideas about the importance of subsurface organisms in early biosphere evolution requires access to a subsurface fossil record. While there have been many reports of microbial fossils from surface and subaqueous environments, examples from subsurface hydrothermal environments have been comparatively few. A specific type of microborings in volcanic glass has been attributed to subseafloor microbial activity (Fisk *et al.*, 1998, 2006), and other examples of fossilized microbes have been reported, for example, from deep basalt aquifers (McKinley *et al.*, 2000). Hofmann and Farmer (2000) recently described a class of filamentous microstructures from subsurface geological settings that were interpreted to be biogenic in many cases.

Subsurface filamentous fabrics (SFF) are here defined as microscopic to macroscopic mineral fabrics that result from the precipitation of minerals on a substrate of filamentous (thread-like) geometric units in subterraneous environments. Typical dimensions of the filamentous units are widths in the range of microns and lengths of hundreds of microns. Filamentous units may be of biological (microbial filaments) or nonbiological (fibrous crystals) origin and may occur in the macroporosity of any type of rock. Filamentous units may show an organization similar to microbial-type mats or vertically draped units. SFF do not include stalactitic speleothems formed from dripping water; these typically have their smallest widths of hundreds of micrometers and are not initiated on top of a solid substrate. Also excluded are microbial fabrics formed in surface environments, but there may occur transitions to these. This particular class of subsurface microstructures has now been recognized from >200 localities worldwide, with a wide range of ages, mineralogies, and geological environments.

Previously explored sites of subsurface microbial activity (Amy and Haldeman, 1997; D'Hondt *et al.*, 2002; Krumholz *et al.*, 1997; Liu *et al.*, 1997; Madsen and Bollag, 1989) often are comprised of porous rocks with only small open spaces, and the rate of microbial growth is generally thought to be very low. A range of other "subsurface" environments that are not entirely closed to the atmosphere provide examples of prolific microbial growth accompanied by the formation of mats and streamers. Such environments include caves (Boston *et al.*, 2001b; Cunningham *et al.*, 1994a, 1994b; Spilde *et al.*, 2001), hot springs in caves (Tazaki *et al.*, 1998), and mine waters (Conrad, 1994; Edwards *et al.*, 2000; Hallberg *et al.*, 2006).

In this paper, we discuss possible biogenic and abiogenic modes of origin of SFF based on geology, morphology, and geochemistry. The value of morphological information in the interpretation of fossil structures has recently been debated, for example, because of the controversy generated by the interpretation of morphological evidence of microfossil-like features in Mars meteorite ALH84001 (*e.g.*, Buseck *et al.*, 2001; Friedman *et al.*, 2001; McKay *et al.*, 1996) but also in the case of the earliest fossils on Earth (Brasier *et al.*, 2002; Schopf *et al.*, 2002). The value of morphology in detecting fossil microbial life has even been dismissed by some authors (Garcia-Ruiz, 2001; Garcia-Ruiz and Amoros, 1998; Garcia-Ruiz *et al.*, 2002). We propose, however, that microbial lifeforms can produce distinctive fabrics structurally organized in ways fundamentally different from abiogenic formations (just as higher life-forms can). In conjunction with supporting geochemical and mineralogical information, morphology over a range of spatial scales may provide an important line of supporting evidence when evaluating biogenicity (Cady *et al.*, 2003).

In view of upcoming planetary explorations, the study of subsurface filamentous fabrics appears particularly important. These features are formed in environments (water-bearing porous rocks of different kinds) that almost certainly were present at some time during the evolution

TABLE 1. EXAMPLES OF SFF OCCURRENCES REFERRED TO IN THIS PAPER

Volcanic-hosted SFF	*Latitude and longitude*	*Type of host material*	*SFF type*
Ebersbach near Colditz, Germany	51°6.18′N, 12°42.43′E	Chalcedony/chert in Permian rhyolite	I, M
Höwenegg, Hegau, Germany	47°54.6′N, 8°44.4′E	Natrolite in Miocene melilite-nephilinite	I, M
Kozakov, Czech Republic	50°35.5′N, 15°14′E	Chalcedony in Permian basalts	I, R
Campsie, Scotland	55°59′N, 4°12′W	Chalcedony in Devonian basalt	I, M
Breiddalur, Eastern Iceland	64°50′N, 14°22′W	Quartz varieties in Tertiary basalts	I, M
Kirkjubol, Eastern Iceland	64°50.6′N, 13°51.5′W	Quartz varieties in Tertiary basalts	I, M
Faeroer Islands	62°10′N, 7°W	Chalcedony/chert in Tertiary basalts	I
Moose Island, Bay of Fundy, Canada	45°23′N, 64°05′W	Quartz varieties in Permian volcanics	I
Needles, Texas, USA	29°15′N, 103°46′W	Chalcedony in Tertiary volcanics	I, M
Cady Mountains, California	34°46′N, 116°17′W	Quartz varieties in Tertiary dacite	I, M, PS
Madras area, Oregon, USA	44°21′N, 121°10′W	Chalcedony in Tertiary volcanics	I, M
Ojo de la Laguna, Chihuahua, Mexico	29°29′N, 106°16′W	Chalcedony in Miocene volcanics	I, PS
Paranà Basin, Brazil	29°S, 53°W	Quartz varieties in Late Cretaceous volcanics	I, PS, U
Sidi Rahal, 50 km E Marrakech, Morocco	31°38′N, 7°28′W	Quartz varieties in Mesozoic basalts	I, U, PS
Hayl as Safil massive sulfide deposit, Oman	23°41′N, 56°33′E	Oxidized zone in Cretaceous sulfide ore	I
Ghouzain massive sulfide deposit, Oman	23°27′N, 56°42′E	In chert between pillows, Cretaceous	I
Deccan trap area, India	18°30′N, 73°50′E	Quartz and zeolites in Tertiary-Cretaceous volcanics	I, M
Rakaia Gorge, New Zealand	43°31′S, 171°39.3′E	Quartz varieties in Upper Cretaceous volcanics	I, M
Kerguelen Islands	49°20′S, 69°20′E	Quartz varieties in Tertiary basalt	I
SFF from oxidized ore deposits			
Johanngeorgenstadt, Saxony, Germany	50°26′N, 12°42′E	Quartz, goethite	I, M
Freiberg, Saxony, Germany	50°55′N, 13°20′E	Quartz, goethite	I, M
Herdorf/Siegen, Germany	50°46′N, 7°57′E	Goethite	I, PS, U
Taouz, Morocco	30°54′N, 3°59′W	Goethite	I, PS, U
Tsumeb, Namibia	19°14.3′S, 17°42.6′E	Duftite	I
Ray, Arizona	33°10′N, 110°59′W	Chrysocolla	I, PS
Matagente, Cerro de Pasco, Peru	10°38.5′S, 76°10.5′W	Goethite	I, M
Broken Hill, New South Wales, Australia	31°58′S, 141°28′E	Goethite, coronadite, quartz	I, PS, U
SFF as diagenetic formations			
Agrigento, Sicily, Italy	37°19′N, 13°35′E	Calcite-encrusted filaments on native S	I
Schwarzwasser, Bern, Switzerland	46°51′10″N, 7°23′25″E	Silicified wood from Miocene sediment	I
Saulcy, Jura, Switzerland	47°18′N, 7°09′E	"Stalactites" in pyritized ammonites, Jurassic	PS
Balingen, Baden-Württemberg, Germany	48°14.75′N, 8°51′E	"Stalactites" in pyritized ammonites, Jurassic	PS
SFF in MVT base metal deposits			
Cracow-Silesian MVT-district, Poland	~50°15′N, 19°30′E	Low-temperature sulfide ore in Triassic dolomites	PS, U
SFF in hydrothermal veins			
Menzenschwand uranium mine, Germany	47°50.32′N, 8°2.63′E	Uraninite-preserved filaments in quartz	I, M
Thunder Bay agate mine, Ontario, Canada	48°31′6″N, 89°9′30″W	Chalcedony-quartz veins in Gunflint Fm	I, M, PS
Gairo, 100 km NW Morogoro, Tanzania	6°9′S, 36°52′E	Chalcedony "stalactites"	I, PS

(*continued*)

TABLE 1. EXAMPLES OF SFF OCCURRENCES REFERRED TO IN THIS PAPER (*CONTINUED*)

Volcanic-hosted SFF	*Latitude and longitude*	*Type of host material*	*SFF type*
SFF in palaeokarst			
Warstein, Germany	51°26.3′N, 8°22.1′E	Palaeokarst in Devonian limestones	I, M
Hohenlimburg, Germany	51°20.6′N, 7°34.5′E	Palaeokarst in Devonian limestones	I, M
Hemer, Germany	51°24′N, 7°47.5′E	Palaeokarst in Devonian limestones	I, M
Piz Alv, Switzerland	46°26.4′N, 9°59.7′E	Palaeokarst in Triassic dolomite	I, M
SFF in altered ultramafic rocks			
Wurlitz, Bavaria, Germany	50°15.2′N, 11°58.7′E	Hydrothermally altered serpentinite	I, PS
SFF in impactites			
Ötting, Ries, Germany	58°47′17″N, 10°37′44″E	In cavities in suevite	I

I, irregular filaments; M, matted fabrics; PS, pseudostalactites; R, ropes; U, U-loops.

of Mars. If SFF are biological in origin, they represent an attractive target for exploration on Mars and, possibly, on other planetary bodies. If they are of abiogenic origin, they are likely to be found on Mars, and their origin and the question of how to differentiate them from true microbial fossils will also become relevant. Because SFF can form easily detectable macroscopic fabrics and often are associated with minerals that contrast with those of surrounding rocks, analogous features on Mars may represent relatively visible targets for rover-based exploration.

SFF IN THE LITERATURE

Conspicuous rocks that we interpret as SFF were recognized long ago, and interpretations of them are manifold. The earliest reports known to us are those of Bowerbank (1842), Daubenton, (1782), and Razumovsky (1835), all of whom reported on so-called "moss agates," a subject of later discussions by Brown (1957), Landmesser (1984), and Liesegang (1915). Two general classes of interpretation, biological and nonbiological, emerged early on, but after Liesegang's (1915) publication, nonbiological interpretations were favored. More recently, biological interpretations were given for 4 occurrences in paleokarst environments, 1 each in Germany (Kretzschmar, 1982; Dexter-Dyer *et al.*, 1984), Switzerland (Baele, 1999; Feldmann *et al.*, 1997), Belgium (Baele, 1999), and France (Audra and Hofmann, 2004). Other occurrences of SFF were described from calcite veins in Devonian sediments in Scotland (Trewin and Knoll, 1999), calcite veins in oceanic serpentinite (Milliken, 2001), pillow lavas (Schumann *et al.*, 2004), and hydrothermal veins in granite (Hofmann, 1989; Reitner, 2004). Filamentous structures interpreted as microbial fossils are also known from several volcanogenic massive sulfide deposits and active submarine vents that range in age from Archean to presently active (Duhig *et al.*, 1992; Iizasa *et al.*, 1998; Juniper and Fouquet, 1988; Juniper *et al.*, 1995; Juniper and Sarrazin, 1995; Little *et al.*, 1999; Pracejus and Halbach, 1996; Rasmussen, 2000). The filaments in these occurrences are typically preserved as sulfides and Fe-(hydr)oxides. A biogenic origin for such structures has been advocated without detailed reasoning, and Hopkinson *et al.* (1998) explained similar structures as nonbiological. Closely related to SFF, filaments in cavities within macrofossils were described from several unrelated occurrences, including phosphatized ammonites from Svalbard (Weitschat, 1986) and silicified fossil wood (Braun and Wilde, 2001; Renault, 1896). There are, thus, many reports of single occurrences, but none of the above authors seem to have recognized the very common worldwide occurrence of SFF as a constituent of low-temperature subsurface cavity infills.

Partly filamentous fabrics in terrestrial carbonate-rich soil- and near-surface environments are often described as *Microcodium* (*e.g.*, Stubblefield and Taylor, 1988; Alonso-Zarza *et al.*, 1998; Kosir, 2004). There is no consensus regarding the origin of these structures; but plant roots, actinobacteria, fungi, and cyanobacteria are inferred. A certain overlap with SFF described here cannot be excluded.

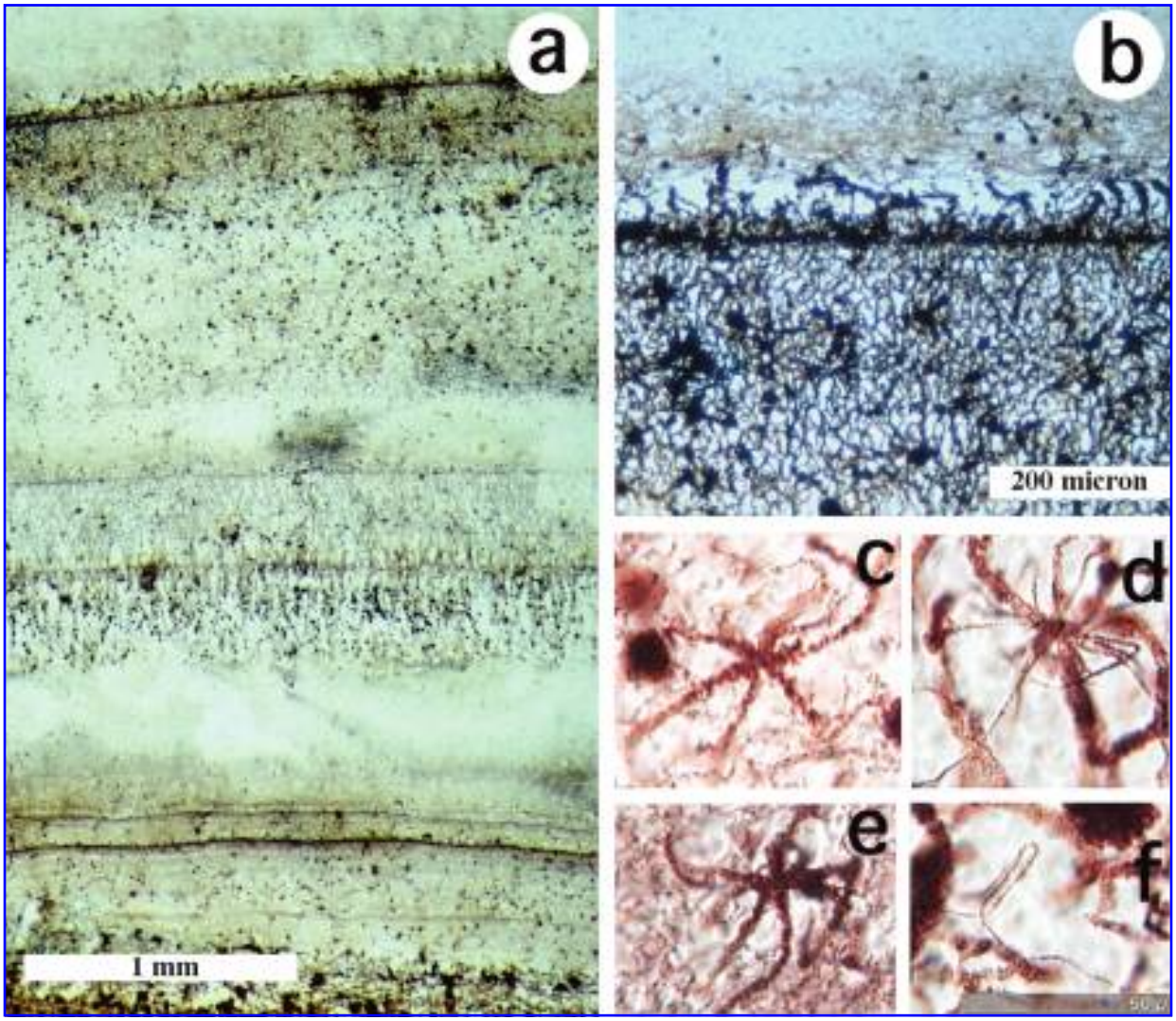

FIG. 1. Sample of microcrystalline quartz from plateau basalts, Kirkjubol, Eastern Iceland. Well-preserved filaments outlined by hematite, NMBE 31339. (**a**) Overview of thin section showing layered, stromatolite-like fabric. Individual traceable layers are as thin as 25 μm. Note preferred vertical orientation of filaments in central part. (**b**) Detail of topmost layer in (a) with high density of filaments. (**c–e**) Star-shaped "Metallogenium"-like features. (**f**) Thin filament with highly variable degree of bending (c–f are at an identical scale).

SAMPLES AND METHODS

Prospection for SFF and sample characterization

Our exploration for SFF started when a slab of polished moss agate from the Cady Mountains, California, attracted our attention at a Swiss mineral show, due to its macroscopic similarity to filament-rich Fe-oxide-rich quartz from Warstein, Germany, which is present in the collections of the Natural History Museum Bern (NMBE) and was described by Kretzschmar (1982). Investigation with a binocular microscope showed the Cady Mountain sample contained a dense network of Fe-oxide encrusted filaments. Based on this initial observation, the mineral collections of the NMBE and others were searched for similar materials, mainly based on macroscopic similarity. Suspicious samples were checked under the binocular microscope for the presence of a filamentous fabric. In many cases, thin sections were prepared, and additional samples were investigated under the scanning electron microscope. Other materials were acquired from mineral dealers and collected during our own fieldwork in the Cady Mountains, in eastern Iceland, and in Piz

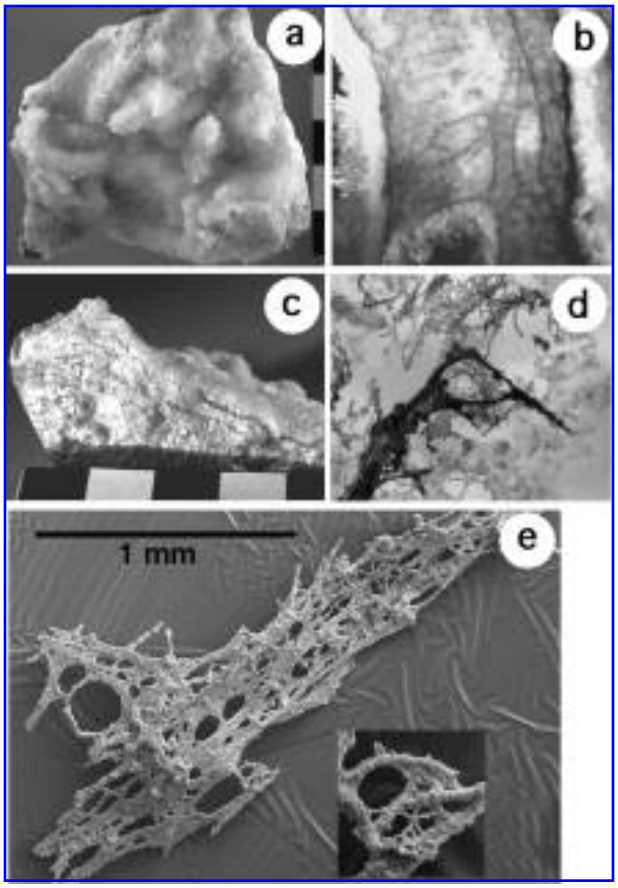

FIG. 2. Sample of natrolite from Miocene melilite-nephelinite, Höwenegg, Hegau volcanics, Germany, NMBE 33559. (**a, c**) Hand specimen displaying needle-shaped natrolite and broken face with dark layered mats. Scale in cm. (**b**) Cut section showing matted fabric, field of view 11 mm. (**d**) Filamentous, sulfide-containing opal obtained by dissolution of natrolite in hydrochloric acid, field of view 1.6 mm. (**e**) SEM image of filamentous opal with detail.

Alv, Switzerland. SFF samples that form the basis of this study are now archived in a special reference collection at the NMBE.

Methods

Detailed investigations, which included filament morphology, were carried out on standard petrographic or polished (0.5 μm diamond grit) thin sections and preparations of hand-picked filamentous materials in immersion oil (n = 1.518). Scanning electron microscopy (SEM) investigations were carried out on unetched and etched samples. Etching was performed by immersion of cm-sized cuttings in 0.1–1% HCl for calcite or in 1–5% HF for chalcedony/quartz. Etching times varied from 1–10 min (HCl) to 1–5 h (HF). After thorough washing in deionized water and drying, samples were coated with a few nm of gold and investigated with the use of a CamScan CS4 SEM. Solid samples of approximately 100 mg of mineralogically homogeneous material (based on visual inspection) to be used for either S or Fe isotope analyses were separated from hand specimens using a wire saw. No further mineral separation was performed. Sulfur isotopes were measured using conventional mass-spectrometric methods (Robinson and Kusakabe, 1975) as SO_2 after combustion of sulfides in Cu_2O at 1075°C and gas purification in a VG SIRA II© isotope ratio mass spectrometer. The precision and accuracy of the isotopic measurements were better than $\pm 0.2‰$ (1σ). Fe isotopes were analyzed after anion-chromatographic purification of iron

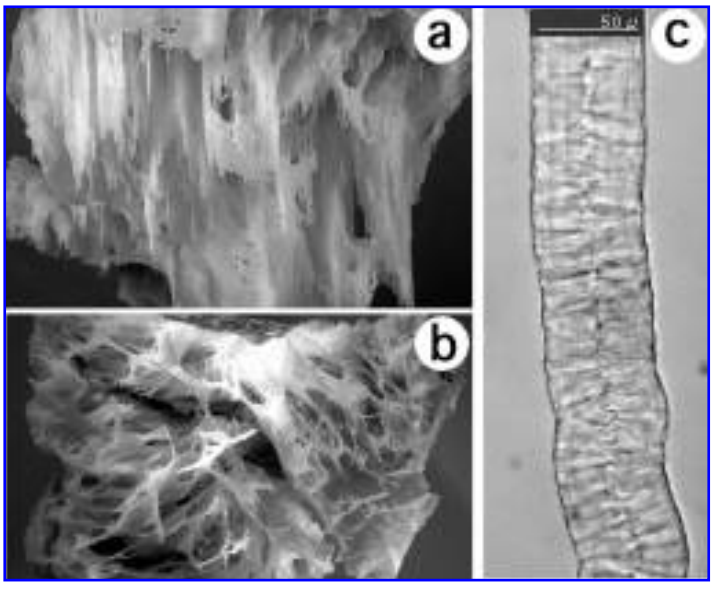

FIG. 3. Sample of chalcedony occurring as thin rods in parallel orientation, from cavity in Mesozoic basalts, Sidi Rahal, Atlas, Morocco, NMBE 35064. (**a**) Hand specimen showing filamentous, vertically draped chalcedony with abundant U-loops, side view (field of view 8 cm). (**b**) Bottom-up view (field of view 10 cm). (**c**) Single chalcedony rod in oil immersion with central channel of ~3 μm.

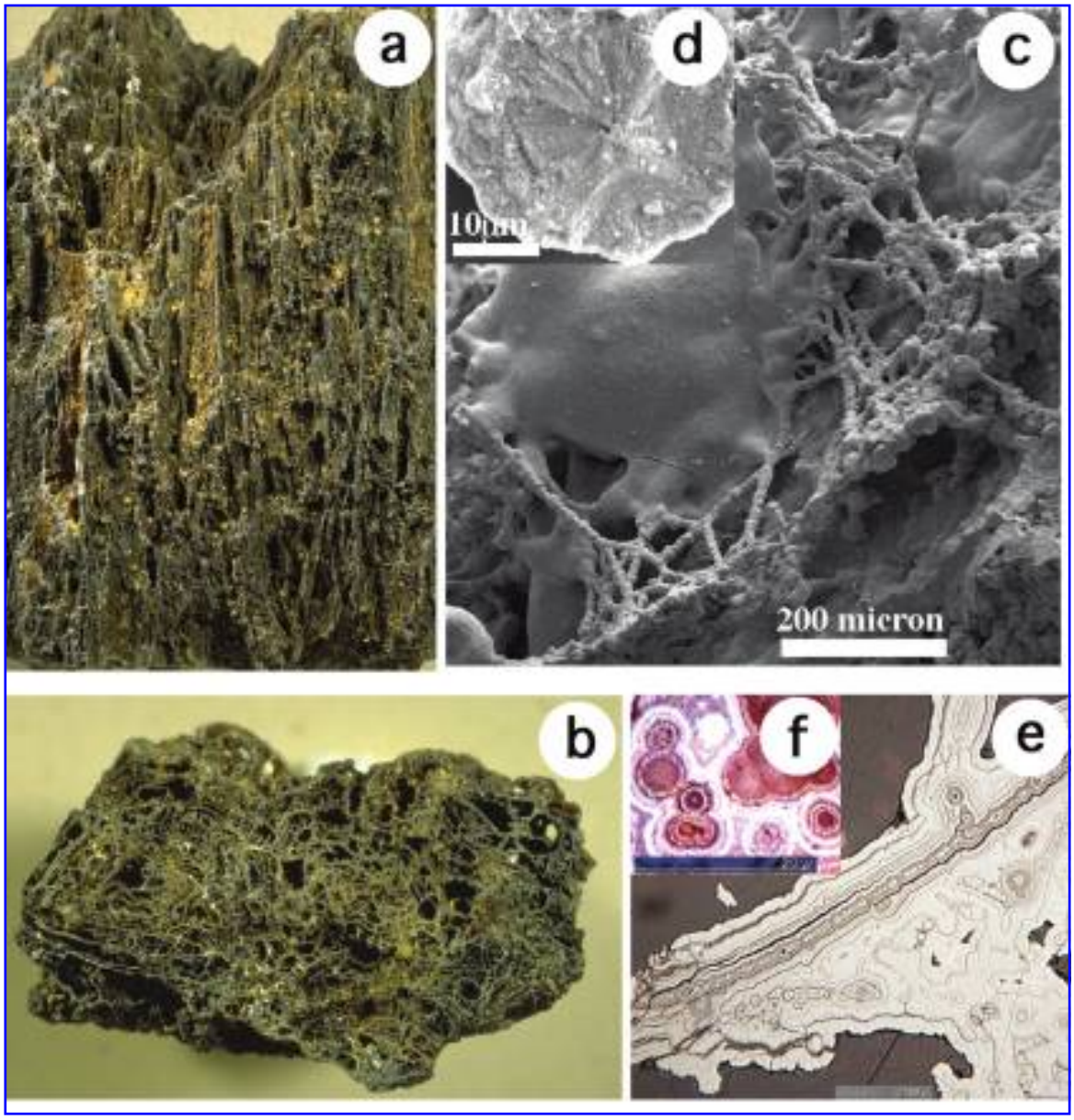

FIG. 4. Goethite with linear fabric from the oxidation zone of the Matagente ore body, Cerro de Pasco, Peru. NMBE 33123. (**a**) Longitudinal section (4 cm wide). (**b**) Cross section (6 cm wide). Texture consisting of a curtain-like arrangement of mats. (**c**) SEM image showing goethite-encrusted filaments in small cavities in (a). (**d**) Goethite-encrusted single filament. (**e**) Reflected light photomicrograph showing goethite-encrusted mat comprising numerous filament cores. (**f**) Same at higher magnification, showing filament cores.

using a Nu-Plasma ICP-MS. The techniques used were the same as given in Walczyk and von Blanckenburg (2002). δ^{56}Fe and δ^{57}Fe ratios are reported relative to the IRMM 14 Fe standard. Reproducibilities (2σ) are 0.1‰ for δ^{56}Fe and 0.15‰ for δ^{57}Fe. Bulk rock geochemistry was determined on chip samples (a few grams each) by instrumental neutron activation analysis (INAA) and, in a more detailed survey, by a combination of INAA and inductively coupled plasma spectrometry (combined ICP-OES and ICP-MS) on powdered samples of homogenized SFF material (representing 20–50 grams each). Analyses were performed by Bondar Clegg (Ottawa, Ontario) and Activation Laboratories (Ancaster, Ontario). For measurements of morphological parameters of microbial filaments collected alive, samples were preserved by adding 2% glutaraldehyde to water from the collection site, and slide mounts with filaments and the same fluid were prepared for transmitted light microscopy. Mineral fibers were similarly prepared with immersion oil.

RESULTS

Occurrences and palaeoenvironments

By the end of 2006, we recognized SFF in samples from 225 localities in 114 different geographical regions on the basis of microscopic analyses given our definition of these structures as noted above. A selection of SFF occurrences mentioned in this paper is listed in Table 1. The most common type of occurrence is in hydrous alteration products in volcanic rocks (57% of localities) and oxidation zones of ore deposits (near-surface gossans to depths of several 100 m, 27% of localities). A lesser number of samples were found in cavities in sediments, often within macrofossils, in Mississippi Valley–Type (MVT) ore deposits and in vein-type hydrothermal mineral deposits in crystalline rocks. In volcanic host rocks, SFF are typically found as inclusions in chalcedony and macrocrystalline quartz filling vesicles, lithophysae, or fractures. Less commonly, SFF are enclosed in opal, zeolites, calcite, or clay minerals. In the oxidation zones of ore deposits, SFF are invariably found as Fe/Mn-hydroxide filaments that paragenetically form one of the oldest precipitates. Very often, hydroxide SFF form the substrate upon which later oxidation-zone minerals, such as cerussite, pyromorphite, vanadinite, hemimorphite, and many others, are precipitated. In general, SFF are found in macroporous rocks that contain low-temperature aqueous alteration assemblages. At present, the only occurrence in rocks of impact origin is in suevites from the Ries crater, even though several other impact sites have been studied where low-temperature alteration products in suevite and melt breccias were abundant (Siljan, Dellen, Sääksjärvi, Sudbury). The classification of environments of formation as subterraneous was based on contextual information obtained in the field (*e.g.*, fracture infills, different kinds of megapores) or on hand specimens (porespace). Macroscopically visible streamer-like, matted, or parallel (pseudostalactitic) fabrics within low-temperature minerals were recognized as good indicators.

Microscopic and macroscopic morphology of SFF

SFF typically consist of filamentous units close to 1 μm in width enclosed, often closely spaced (typical lateral distance of subparallel filaments is a few to a few tens of micrometers), in later mineral cements that partially or completely filled palaeocavities (Figs. 1–4). Three characteristic fabric types can be identified in SFF: irregular masses of filaments, planar geometries (matted fabrics), and vertically draped elements that resemble stalactites (pseudostalactites). *Tubular filaments* are found in unorganized association. Such occurrences may represent primary structures or filament debris. *Matted fabrics* consist of filaments aligned in high density in a plane; these fabrics sometimes resemble stromatolites (Fig. 1). *Pseudostalactites:* In many SFF samples, filament assemblages show vertically oriented fabrics, often very similar to stalactites (Figs. 3, 4). Vertically arranged fabrics contain the full range of transition features between linear pseudostalactites and 3-dimensional textures that appear similar to curtains of folded fabric. In contrast to stalactites, where the primary width of the structures is controlled by the size of water drops (2–9 mm width), which result in so-called soda-straw stalactites of similar width (Hill and Forti, 1997), the smallest width of the vertically arranged fibrous fabrics described here is $<<1$ mm and often on the order of micrometers (in poorly preserved cases 10–50 microns), inconsistent with a stalactitic origin. Numerous randomly oriented filaments were often observed in the center of the structures we examined. Even pyritized fossils (such as the pyrite stalactites we have found in ammonites from upper Jurassic clays in Switzerland and southern Germany) can sometimes contain cavities with pseudostalactites (Hudson, 1982). Besides consisting of vertically oriented elements, pseudostalactites were often found associated with features whose origin could be explained by gravity draping of initially flexible filament strands (U-loops). The convex side of U-loops points in the same direction as pseudostalactites, which confirms gravity control. While at some localities only 1 of the 3 forms of filament textures (filaments, matted fabrics, pseudostalactites) has been observed, many localities show the occurrence of all 3 types. Examples of SFF fabrics are shown in Figs. 1–4.

SFF containing structures resembling Gallionella *and "Metallogenium"*

At 2 localities (volcanics of the Breiddalur area in eastern Iceland and palaeokarst of Warstein, Germany), filamentous SFF (dominantly matted fabrics) are associated with coiled ribbons of Fe

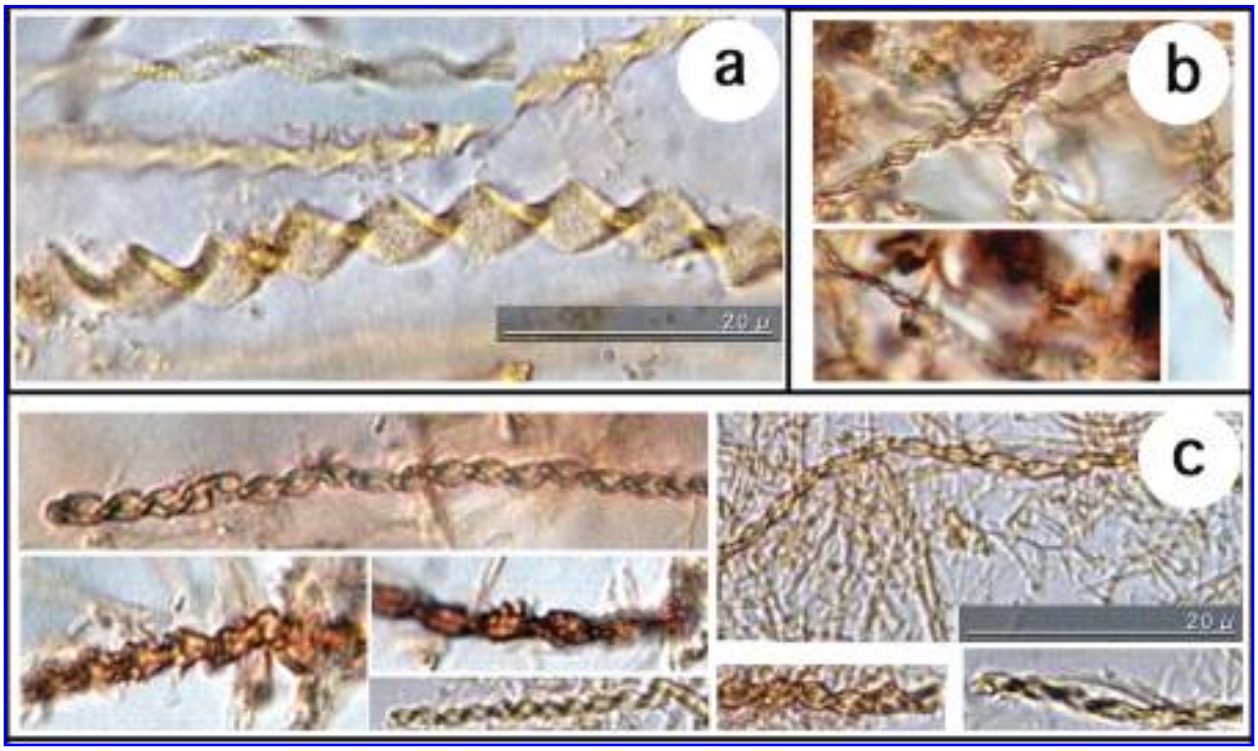

FIG. 5. ***Gallionella*-like twisted Fe-hydroxide stalks from fossil SFF occurrences and an active spring.** (**a**) In chert from Miocene plateau basalts, Breiddalur, Eastern Iceland, NMBE 33089. (**b**) Enclosed in megaquartz from palaeokarst, Warstein, Germany, NMBE 30436. (**c**) From an active, Fe-hydroxide–depositing underground spring in the Gonzen Mine, Switzerland. All images shown at the same scale.

hydroxide that strongly resemble the characteristic extracellular stalks produced by *Gallionella*, an iron-oxidizing bacterium that is common in recently active sites with Fe-rich water under neutral or slightly acidic pH and moderately oxidizing conditions (Banfield *et al.*, 2000; Ellis, 1919; Ferris *et al.*, 1999; Hallbeck and Pedersen, 1995; Hallbeck *et al.*, 1993; Molisch, 1910). The morphology of the fossil stalks is virtually identical with *Gallionella* stalks collected in active Fe-rich springs in mines (Fig. 5). The width of the stalks is variable even within a single occurrence (Fig. 5c). At Breiddalur, Eastern Iceland, *Gallionella*-like stalks occur, along with filaments that are similar to those found in other occurrences of SFF, in cavity infills that consist of microcrystalline quartz-chalcedony. This material occurs regionally in palaeocavities within basalt and andesite of an 8 Ma regional volcano (Feucht, 2006; Feucht *et al.*, 2006; Hofmann and Farmer, 2000).

Star-shaped filamentous structures that resemble "Metallogenium," a morphotype of uncertain affinity that is possibly related to Mn-oxidizing bacteria (Dubinina, 1970; Klaveness, 1977; Zavarzin, 1981), were found within a finely laminated, matted fabric with well-preserved filaments in a cavity infill consisting of microcrystalline quartz at Faskrudsfjördur in eastern Iceland (Fig. 1c–1e).

Comparison of filamentous fabrics with microbial filaments and mineral fibers

To compare the morphology of filaments in SFF with possible biological and nonbiological precursors, 4 morphological parameters were measured in suites of samples that contained the following: (I) certain microbial filaments; (II) natural abiogenic fibers, selected from widely different environments to represent a comprehensive abiological sample; (III) SFF. Morphometric data are summarized in Table 2 and Figs. 6 and 7.

Abiogenic samples were intentionally selected to represent fiber widths in the same range as the widths of the microbial filaments studied to obtain a nonbiological sample that would represent potential precursors. The median width of 2.1 μm of abiogenic fibers, relatively close to that of SFF (1.7 μm), is thus a result of this intentional selec-

tion. Abiogenic samples include asbestiform fibrous minerals, whisker crystals of native silver and halotrichite, and fibers of volcanic glass. The mineral fibers were chosen to represent a wide range of abiogenic shapes. The assumption of an abiogenic nature of these fibers is based on the inferred temperature of formation, the mode of occurrence (often as highly organized parallel or radial fibers, or whiskers), or a combination of these factors. Measured biological filaments included mainly uncharacterized filamentous microorganisms from various environments, which were preserved with 2% glutaraldehyde. Data for actinomycetes were obtained from Fig. 16.103 in Madigan *et al.* (1997). We are aware that the biological and nonbiological samples selected for morphological analysis comprise only a limited subset of all possible representatives, but we believe they capture a reasonable range of examples.

The four morphological parameters determined are filament/fiber widths, bending, tortuosity, and number of direction changes per unit length. These parameters were measured on 12 microbial filament samples collected alive (158 filaments), 13 abiogenic fiber samples (162 fibers), and 11 SFF samples (168 filaments). In digital images, filaments were digitized into coordinate trains using NIH Image software. Bending (= curvature, °/μm), number of direction (sense of bending) changes per mm, and tortuosity (length of filament from beginning A to end B/straight line A–B) were then calculated for each digitized filament/fiber. Because the data are not or only partly normally distributed, median values (and the quartiles $Q_{.25}$ and $Q_{.75}$) obtained from individual measurements of all filaments will be discussed as summary parameters. In addition to the SFF filaments measured for all parameters, widths only were determined for 23 additional SFF samples (total of 840 measurements).

Filament widths: The median width of the 359 morphologically investigated SFF filaments (Table 2) is 1.7 μm ($Q_{.25}$ 0.8, $Q_{.75}$ 2.5 μm), the larger sample of 840 filaments yields 1.6 μm ($Q_{.25}$ 1.0, $Q_{.75}$ 2.4 μm). Median values for samples from different environments, *e.g.*, oxidation zones ($Q_{.5}$ 1.2 μm, $n = 109$) and volcanic-hosted environments ($Q_{.5}$ 1.5 μm, $n = 390$), are very similar. Abiogenic fibers, selected for a similar width as SFF, have a slightly larger median width of 2.1 μm but also a larger variability ($Q_{.25}$ 0.7, $Q_{.75}$ 5.0 μm). Microbial filaments have a median width of 2.0 μm ($Q_{.25}$ 1.5, $Q_{.75}$ 2.6 μm) and are thus very similar to the SFF population. Histograms of the widths for the 3 populations (Fig. 6) show that microbial and SFF filaments show relatively narrow peaks while the abiogenic fibers are characterized by a very different, skewed distribution.

Bending (degrees/micron): For abiogenic fibers, bending values are low with a median of 0.15 ($Q_{.25}$ 0.04, $Q_{.75}$ 0.38). Both microbial filaments and SFF have higher median values of 0.87 and 2.5, respectively, and broader distributions.

Direction changes (n/mm): Most abiogenic fibers show very low values (median 0.0). Only glass fibers and native silver show slightly elevated values, though they are still lower than those for microbial filaments ($Q_{.5} = 25$) and SFF ($Q_{.5} = 73$).

Tortuosity: Median values for abiogenic fibers, microbial filaments, and SFF are similar (<1.1). While the range for microbial filaments and SFF is somewhat larger, the 3 populations do not appear to be very different.

The "bending" and "number of direction changes" parameters differentiate between abiogenic fibers and microbial filaments and even more strongly between abiogenic fibers and SFF. In a plot of bending versus direction changes (Fig. 7), abiogenic fibers cluster close to the origin, while microbial filaments and SFF show much larger variations and a lot of overlap. For microbial filaments and SFF, the 2 parameters are highly correlated ($r = 0.89$ and 0.82). Based on these data it is concluded that the morphologies of SFF and abiogenic fibers are different. Microbial filaments are somewhat intermediate between the abiogenic and SFF populations. The general characteristics of both microbial filaments and SFF are a high degree of bending and a high number of direction changes, combined with very similar widths. Compared to this, abiogenic fibers show less bending and direction changes; their median width is again similar but widths show a different distribution.

Multivariate statistical analysis demonstrates that 2 factors explain the majority of variations. A plot of factor 1 versus factor 2 shows a large overlap between biogenic filaments and SFF. SFF and abiogenic fibers show most differences.

Preservation of organic matter

Based on microscopy and hydrofluoric acid digestion of many samples of SFF, filaments usu-

TABLE 2. MORPHOMETRIC DATA FOR FILAMENTOUS/FIBROUS SHAPES

Microbial filaments	*Bending*	*Tortuosity*	*D-changes*	n	*Width*	n
Baden, Switzerland (BA5a)	1.32	1.1	78.0	10	1.5	38
Baden, Switzerland (deep)	0.61	1.22	5.9	9	1.4	9
Gonzen, Switzerland Feox	0.57	1.1	14.8	14	1.9	51
Gonzen, Switzerland Sox	0.64	1.24	10.1	12	2.2	27
Mammoth hot springs	1.29	1.09	54.2	19	1.3	21
Nack, Germany (fine)	0.83	1.09	30.1	9	1.7	62
Nack, Germany (coarse)	2.01	1.07	32.4	14	2.5	70
NMBE "slime" (B)	0.51	1.14	15.8	16	2.9	41
NMBE "slime" (A)	0.31	1.03	14.3	10	3.3	20
Grimsel, Switzerland	0.44	1.07	10.0	19	1.9	44
Actinomycetes	15.4	1.43	344.0	11	1.0	44
Fungal growth in lab	1.82	1.07	67.1	15	3.4	44
$Q_{.25}$	0.48	1.04	10.7		1.5	
$Q_{.5}$	0.87	1.09	24.8		2.0	
$Q_{.75}$	1.71	1.35	57.7		2.6	
Inorganic filament-like forms						
Glass fibers from brimstone	0.17	1.01	7	12	4.4	58
Jamesonite McLoughlin	0.02	1.01	0	7	6.0	43
Mordenite A9472	0.04	1.00	4	10	3.6	78
Tourmaline A9119	0.19	1.03	0	15	1.2	72
IS4 mordenite	0.04	1.00	0	7	5.6	46
Actinolite asbestos 1448	0.08	1.00	0	21	2.7	80
Chrysotile asbestos 3957	0.01	1.00	0	11	2.4	50
Crocydolite asbestos	0.21	1.08	0	20	0.7	56
Native silver 238	1.06	1.75	10	11	8.2	50
Halotrichite A8721	0.05	1.02	2	12	3.8	42
Goethite 31224	0.65	1.00	0	10	0.5	126
Todorokite	0.43	1.18	0	14	0.6	75
Aragonite	0.03	1.01	0	12	4.6	75
$Q_{.25}$	0.04	1.00	0.0		0.7	
$Q_{.5}$	0.15	1.01	0.0		2.1	
$Q_{.75}$	0.38	1.10	4.5		5.0	
Subsurface filamentous fabrics SFF						
Oman1 (HS)	4.61	1.12	99	16	2.6	50
Oman20 (Ghuzain)	4.67	1.10	134	14	2.0	59
Cady C18	0.98	1.04	27	22	0.6	29
Iceland IS10	3.05	1.22	80	19	2.1	49
Tsumeb (B79776)	1.4	1.03	59	12	2.3	23
Warstein, Germany	4.56	1.10	151	16	1.1	22
Piz Alv, Switzerland	2.07	1.10	74	16	0.6	28
Paranà Basin, Brazil (B7000)	1.92	1.07	66	10	3.5	25
Madras, Oregon (OR13)	2.79	1.05	78	12	0.7	30
Hohenlimburg, Germany	2.95	1.08	93	15	0.6	27
Campsie, Scotland	1.84	1.11	61	16	1.4	17
$Q_{.25}$	1.52	1.05	49		0.8	
$Q_{.5}$	2.5	1.09	73		1.7	
$Q_{.75}$	4.65	1.17	130		2.5	

SFF widths based on all measurements ($n = 840$); $Q_{.25} = 1.0$, $Q_{.5} = 1.6$, $Q_{.75} = 2.4$.

ally do not appear to contain residual organic matter, which implies complete oxidation shortly after entombment. This preservational mode is typical of oxidizing, subaerial thermal springs in Yellowstone National Park (Cady and Farmer, 1996; Farmer, 1999a) and has also been reported from comparable Devonian-aged siliceous sinters from northeast Queensland, Australia (Walter *et al.*, 1996, 1998). In 2 cases, organic matter was detected in filaments: (1) a sample from Hohenlimburg, Germany, in which filaments are enclosed in megaquartz and (2) a sample of silicified wood from Switzerland where organically preserved filaments are present in fractures along with in-

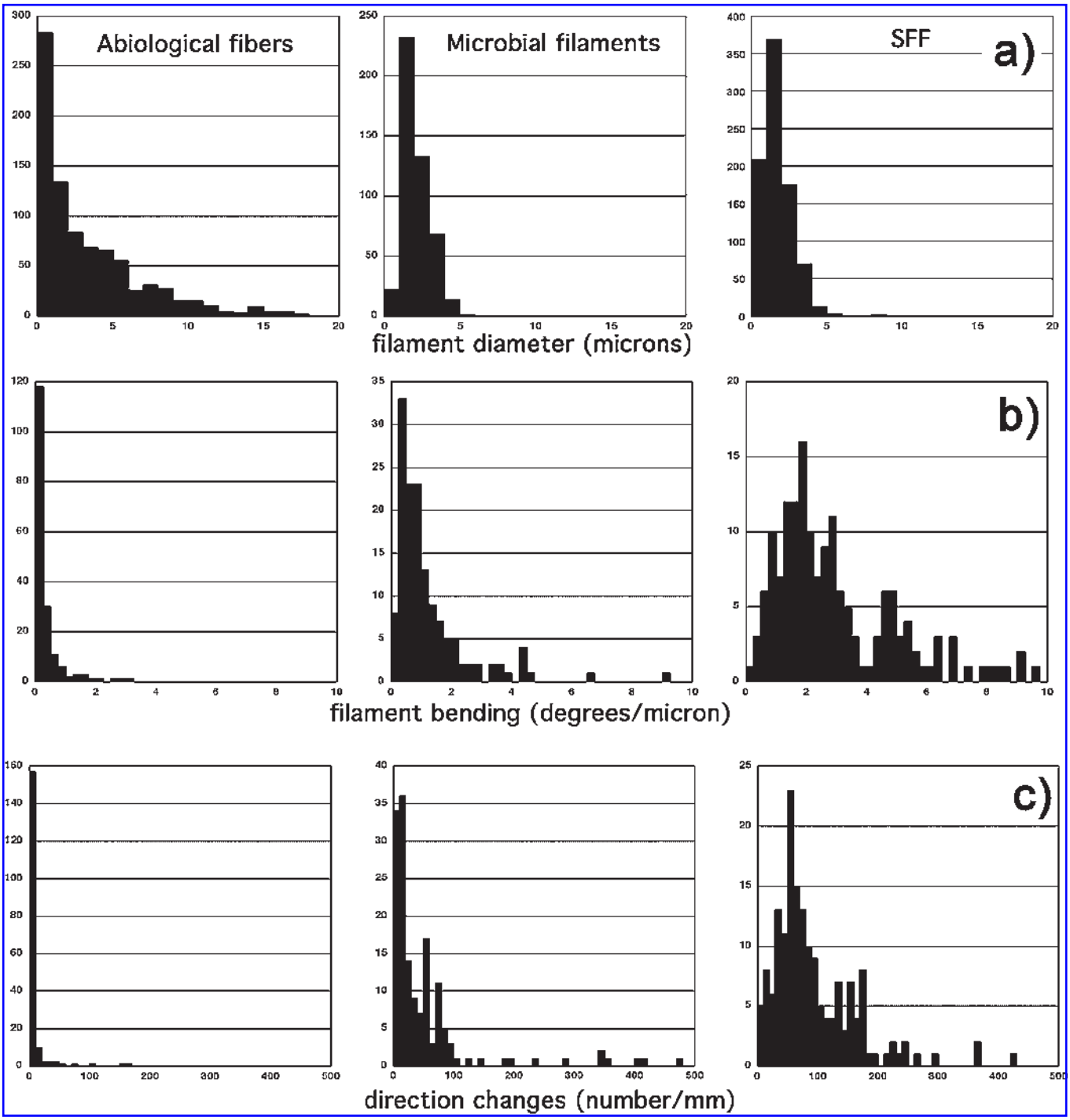

FIG. 6. Histograms of morphological parameters determined for abiological fibers, microbial filaments, and filamentous forms from SFF. (**a**) Widths—note similarity of distribution between microbial filaments and SFF while abiological forms have skewed distribution. (**b**) Bending in abiological fibers is dominantly very low compared with microbial filaments and SFF. (**c**) Direction changes show a similar pattern as that observed with bending.

organic preservations (Fig. 8); the silicified wood sample provided a basis for direct comparison of inorganic filamentous fabrics and organically preserved filaments. In both cases the presence of organics was confirmed by Raman spectroscopy.

Mineralogy and modes of preservation

The mode of cementation of SFF fabrics by minerals is similar in most observed localities and summarized in the following. We assume that all

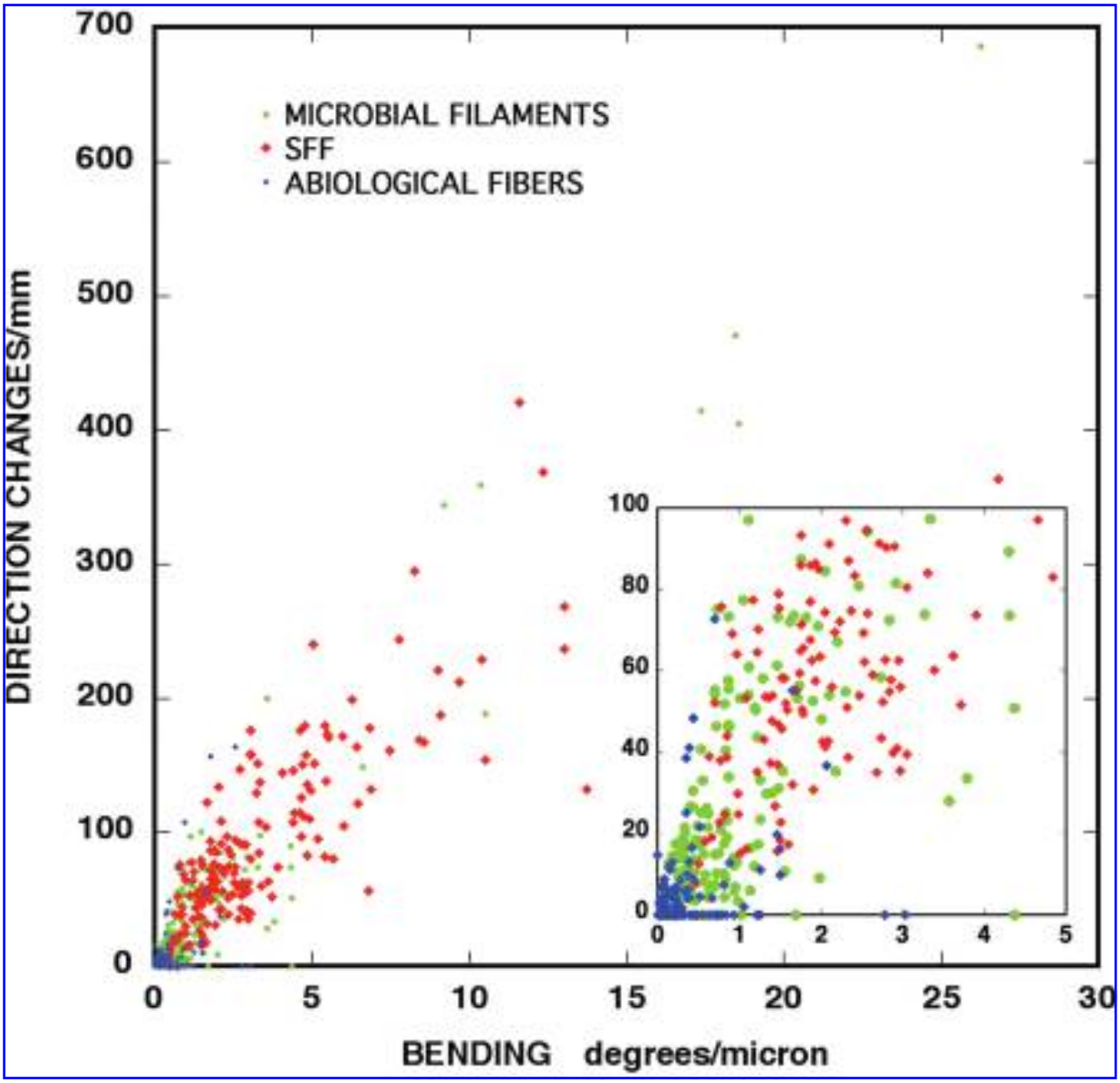

FIG. 7. Plot of bending versus direction changes for microbial filaments collected alive (green circles), abiogenic filament-like fibers (blue diamonds) and filamentous forms from SFF (red diamonds). This plot shows the data for all measurements of single filaments/fibers. Abiological fibers (n = 851) occupy a field close to zero bending and direction changes, while microbial filaments (n = 471) and SFF (n = 359) are spread over a wide area, often with high values, and generally occupy the same field.

cementation processes were largely nonbiological, even when assuming a biogenic origin for the filamentous substrate. Most commonly, SFF are preserved due to encrustation by Fe hydroxides. The delicacy of preservation appears to depend on the timing of subsequent cementation by other minerals (most commonly quartz). Filament preservation was most detailed in cases where cementation by SiO_2 occurred early, before much Fe hydroxide had been precipitated. In our samples, goethite is very common, while hematite occurs at a minority of localities only, which is probably a reflection of the general low-temperature nature of SFF-containing mineral cements. In addition to Fe hydroxides, filaments may also be preserved in quartz (with accompanying variation of grain size) and, rarely, by replacement with sulfides. In a second phase of cementation, a range of different minerals may be precipitated in the open space between filaments, including quartz, chalcedony, calcite, zeolites, and massive Fe (hydr)oxides. Often, a later replacement of

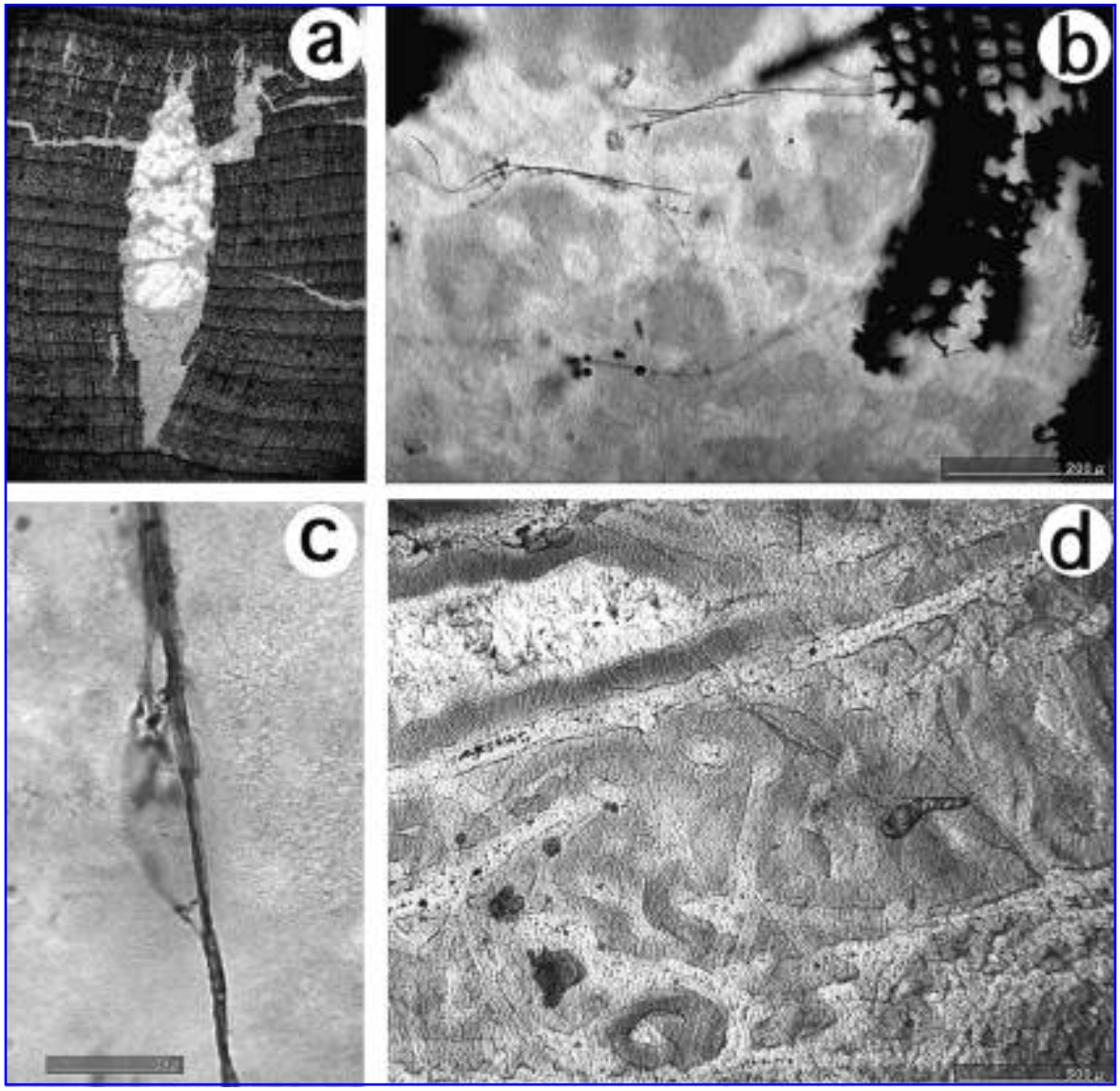

FIG. 8. Silicified wood from Miocene shallow marine Molasse sediments, Schwarzwasser area, Bern, Switzerland, NMBE D3116. (**a**) Chalcedony-filled cavity containing organically preserved filaments (field of view 4 mm). (**b**) Organically preserved filaments in chalcedony. Some filaments are decorated with pyrite (black). Note attachment of filaments to structurally different cellular wood material. (**c**) Detail of organically preserved filament. (**d**) Completely mineralized filaments devoid of organic carbon from the same specimen. Filament remnants are decorated with pyrite and show encrustations by several generations of chalcedony.

early Fe hydroxides by Fe-rich celadonitic clays can be observed. Typically, yellow-brown Fe hydroxides are replaced by celadonitic clays along fractures and zones of high porosity. During replacement of Fe hydroxides by Fe-rich clays, morphological details are mostly lost. The same is the case where major recrystallization occurred during precipitation of secondary phases. The occurrence of goethite (α-FeOOH) as an early phase that encrusts filaments provides evidence that, during that early stage, temperatures did not significantly exceed 100°C (Diakonov *et al.*, 1994). Preservation of filaments enclosed in quartz was observed even in the feeder zone of a massive sulfide deposit in Oman where temperatures close to 300°C were likely reached after filament entombment. This is consistent with the generally observed temperature stability range of quartz during diagenesis.

Elemental geochemistry of SFF host materials

Samples of subsurface mineral precipitates that contain filamentous fabrics (SFF) were analyzed

TABLE 3. INAA DATA FOR SFF CHIP SAMPLES (MEAN VALUES)

	n	*Sc*	*Fe* (%)	*As*	*Sb*	*W*	*Au* (ppb)	*U*	*As/Sb*
Paranà Basin, Brazil (V)	2	<0.1	0.1	0.25	0.05	<1	69	<0.2	
Sri Lanka (V)	1	<0.1	0.1	13	23	<1	<2	<0.2	0.6
Rakaia Gorge, New Zealand (V)	3	<0.1	0.2	0.5	0.4	<1	3	1.2	1.3
Indian moss agates (V)	6	<0.1	0.3	<0.5	<0.2	2	<2	<0.2	
Needles, Texas, USA (V)	1	<0.1	0.3	4.2	0.2	<1	<2	1.9	21
No locality	1	1	0.6	6	3.4	<1	100	<0.2	1.8
Kerguelen Islands (V)	2	0.62	0.7	1.4	0.05	<1	<2	<0.2	>28
Kozakov area, Czech Republic (V)	6	0.75	1.1	32	37	2	11	0.7	0.9
Priday Ranch, Oregon, USA (V)	7	0.44	1.3	14	2.5	1.5	<2	2.8	5.7
Ojo Laguna, Mexico (V)	1	0.9	1.4	18	0.7	<1	<2	3.7	26
Quegstein, Germany (V)	1	<0.2	1.5	6	0.4	<1	6	10	13.8
Hemer, Germany (P)	2	<0.2	2.3	8	19	<1	<2	0.2	0.4
Eastern Iceland (V)	6	2	3.2	1.7	0.2	1	2	<0.2	8.5
Warstein, Germany (P)	1	0.23	3.5	9	9.2	<1	<2	0.25	1.0
Johanngeorgenstadt, Germany (O)	2	2.4	3.6	377	22	270	<2	40	17
Freiberg, Saxony, Germany (O)	1	0.6	4.9	600	1080	8	<2	12	0.6
Faeroer Islands (V)	1	5.8	5.2	0.65	0.18	<1	8	0.5	3.6
Moose Island, Bay of Fundy, Canada (V)	1	10	7.3	40	0.6	1.7	<2	2.8	67
Cady Mountains, California (V)	21	2.5	18.4	1477	147	9.1	<2	3.6	10.0
Average upper crust[a]		11	3.5	1.5	0.2	2	1.8	2.8	7.5

All values ppm unless otherwise noted; sample suites are arranged with increasing Fe content.
Th <0.2 ppm except for Moose Bay: 0.7 ppm.
All data from chips of a few g mass to avoid contamination during powder preparation.
Types of SFF occurrences: V, hosted in volcanic rocks; O, oxidation zones; P, palaeokarst.
[a]After Taylor and McLennan (1985).

for trace elements with the intention of characterizing the geochemical environments of formation. Initially, 66 chip samples (typically 1–5 g) from 19 localities were analyzed by INAA. In a second phase, 29 samples from 12 localities were fully characterized using combined INAA, ICP-OES, and ICP-MS methods. Data are given in Tables 3 and 4. INAA data demonstrate that SFF are strongly depleted in the immobile element Sc due to the predominance of aqueous precipitates, mainly quartz varieties that are low in immobile elements (Table 3). Samples from basaltic host rocks (Iceland, India, New Zealand, Kerguelen) often show low concentrations of trace elements. Many samples show a strong enrichment of highly mobile As and Sb, and some of W, which is consistent with their origin related to the circulation of hydrothermal fluids. As and Sb show the strongest enrichment relative to average crust. Detailed geochemical characterization (Table 4) confirmed high concentrations of As and Sb for many occurrences and indicated strong enrichments in Mo, Be, and V relative to depleted immobile elements (Al, Sc, La). The As/Sb ratio is highly variable (0.4–75, median 9.4), but values were in the range of As/Sb observed for thermal waters as in Yellowstone Park [19–123, mean 49, (Stauffer and Thompson, 1984)] and sea water [11.3 (Taylor and McLennan, 1985)]. Fe abundances ranged from 0.25 to 20.9% but were always enriched relative to immobile Sc and average continental crust, which confirmed that this element plays an important role in environments that host SFF. The enrichment of Fe can be explained by oxidation of dissolved ferrous iron in most cases. The Cady Mountains, California, occurrence is characterized by particularly elevated concentrations of many elements. Even when this site is excluded , there remains a clear positive correlation of many elements (P, V, Mn, Ni, Zn, As, Sb) with Fe, probably due to the well-known ability of Fe-minerals to adsorb and

TABLE 4. GEOCHEMISTRY OF SFF MATERIALS II: DETAILED ANALYSES OF POWDER SAMPLES (MEAN VALUES)

	n	*Be*	*Al* (%)	*P*	*K* (%)	*Ca* (%)	*Sc*	*V*	*Mn*	*Fe* (%)	*Ni*	*Fe/Mn*
Indian moss agate (V)	2	<1	0.16	<10	0.13	0.08	0.2	15	62	0.25	4	40
Eastern Iceland natrolite (V)	2	<1	3.12	<20	0.03	5.56	0.5	5	65	0.70	11	106
Needles, Texas (V)	1	1	0.6	<10	0.27	0.03	0.5	6	14	0.92	2	637
Thunder Bay, Ontario (V)	1	<1	0.05	<10	0.02	0.89	0.1	4	419	0.94	10	22
Lake Superior agates (V)	4	<1	0.16	33	0.04	0.04	0.5	24	219	1.40	14	64
Madras, Oregon (V)	3	1.5	0.28	60	0.19	0.09	1.4	150	280	1.45	20	52
Campsie, Scotland (V)	1	1.1	0.10	20	0.06	4.00	1.6	57	26	1.74	7	671
Ebersbach, Germany (V)	1	<1	0.02	20	0.01	<0.01	0.3	11	53	2.38	5	447
Piz Alv, Switzerland (P)	3	6	0.02	20	<0.01	0.02	0.2	33	17	4.61	9	2730
Bay of Fundy, Nova Scotia (V)	1	<1	1.81	15	0.34	1.34	8.5	71	374	8.7	34	232
Bahia, Brazil (P)	1	1.3	0.24	43	0.02	0.10	0.5	245	242	9.28	35	384
Eastern Iceland (V)	2	<1	0.44	18	0.04	1.91	6.9	138	527	9.87	23	187
Cady Mountains, California (V)	9	43	0.19	40	0.06	4.73	1.5	74	1538	20.91	32	136
Upper continental crust[a]		3	8.00	1050	2.82	3.0	11	60	600	3.5	20	58

	Cu	*Zn*	*Ge*	*As*	*Sr*	*Y*	*Mo*	*Sb*	*Ba*	*La*	*Au* (ppb)	*As/Sb*
Indian moss agate (V)	5	5	<0.1	0.5	9	<1	<1	0.1	50	0.5	<2	5.0
Eastern Iceland natrolite (V)	14	6	<0.1	1.1	381	<1	<1	<0.1	50	0.5	<2	11.0
Needles, Texas (V)	7	1	<0.1	5.3	5	<1	1.5	<0.1	50	0.5	<2	53.0
Thunder Bay, Ontario (V)	17	6	<0.1	9.9	8	1	2.3	0.3	50	0.5	13	33.0
Lake Superior agates (V)	86	7	<0.1	5.7	8	4	4.1	0.4	113	1.2	1	13.4
Madras, Oregon (V)	10	8	<0.1	7.1	11	3	2.5	1.6	67	3.3	<2	4.4
Campsie, Scotland (V)	9	52	<0.1	60	18	2	2.5	0.8	50	0.8	<2	75.4
Ebersbach, Germany (V)	6	2	<0.1	43	5	5	18.3	1.6	450	5.0	<2	26.7
Piz Alv, Switzerland (P)	5	9	1.7	386	6	1	15.3	29.4	50	0.5	<2	13.1
Bay of Fundy, Nova Scotia (V)	20	19	<0.1	51	65	15	6.4	1.0	300	4.9	<2	51.2
Bahia, Brazil (P)	22	87	<0.1	56	6	2	<1	6.4	130	1.5	10	8.8
Eastern Iceland (V)	33	9	0.1	6.5	24	7	0.9	0.3	95	1.8	<2	25.8
Cady Mountains, California (V)	35	293	0.6	1429	147	9	167	193	401	6.5	<2	7.4
Upper continental crust[a]	25	71	1.6	1.5	350	22	1.5	0.2	550	30	1.8	7.5

All values ppm unless otherwise noted; sample suites are arranged with increasing Fe content.
Types of SFF occurrences: V, hosted in volcanic rocks; O, oxidation zones; P, palaeokarst.
[a]After Taylor and McLennan (1985).

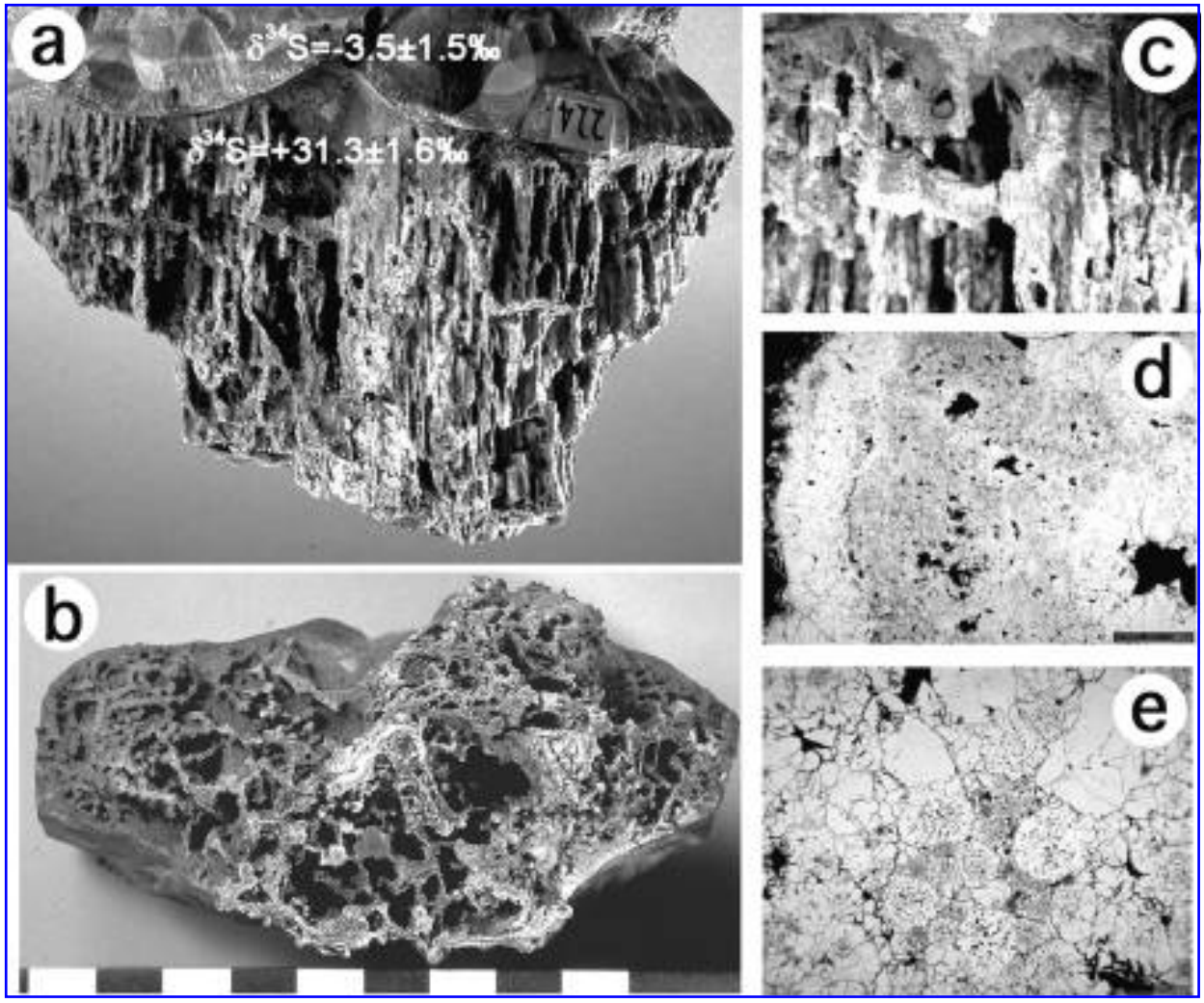

FIG. 9. Sulfide sample from the Cracow-Silesian MVT lead-zinc district, Poland, NMBE 35067. Sulfur isotope data (Table 5) for this sample show a strong increase of $\delta^{34}S$ just below the textural boundary. The fabric is similar to that of goethite in Fig. 4. (**a**) Oblique view of hand specimen consisting of isotopically light botryoidal sphalerite (top) containing minor galena and vertically draped, isotopically light pseudostalactitic marcasite/pyrite below. (**b**) Bottom-up view, cm scale. (**c**) Detail showing U-loops (field of view 3 cm). (**d**) Cross-section of vertically arranged stalk with core of framboidal pyrite and rim of marcasite, reflected light. (**e**) Detail of framboidal pyrite, reflected light.

concentrate trace metals. In most cases, Fe/Mn ratios are above crustal values, which demonstrates the association of SFF with Fe rather than Mn enrichments.

Sulfur isotopes

Sulfides typically are scarce or absent in most examples of SFF. In chalcedony-rich samples, which dominated SFF occurrences studied here, traces of sulfides were only rarely observed. However, filamentous and stalactitic features that closely resemble SFF are known from MVT deposits [*e.g.,* from Wiesloch, Germany (Lieber, 2001)] and sulfide-rich diagenetic precipitates. In sulfide-rich samples, however, filaments are never as well preserved as they are in silica. We have investigated a sulfide specimen from an MVT deposit in the Cracow-Silesian Pb-Zn district, Poland. This sample consists of botryoidal sphalerite/galena with later overgrowths of "stalactitic" pyrite/marcasite (Fig. 9). Based on the descriptions by Leach *et al.* (1996a), the botryoidal sphalerite-galena corresponds to paragenetic stage 3 of the district-wide correlatable mineral sequence. While speleothem-like fabrics are re-

Table 5. Sulfur Isotope Data for "Stalactitic" MVT Sulfide Sample from Poland

	mm[a]	$\delta^{34}S$	
PL1	−2	−1.1	sphalerite
PL15	−4	−4.6	galenite
PL2	−7	−2.4	sphalerite
PL3	−11	−3.5	sphalerite
PL14	−13	−3.3	galenite
PL4	−15	−3.2	sphalerite
PL5	−19	−3.1	sphalerite
PL6	−23	−2.7	sphalerite
PL7	−26	−3.8	sphalerite
PL8	−29	−6.9	sphalerite
PL9	−30	−32.5	marcasite
PL10	−40[b]	−30.7	marcasite
PL11	−40[b]	−32.9	marcasite
PL12	−40[b]	−31.5	marcasite
PL13	−40[b]	−28.8	framboidal pyrite

[a]Position of sample in mm below profile start.
[b]Position approximate (distances overlapping).

ported (Leach *et al.*, 1996b; Motyka and Szurawinski, 1989), the paragenetic sequence appears unclear. The "stalactitic" fabric in our specimen is similar to SFF from volcanic environments and oxidation zones. The vertically oriented pyrite/marcasite pseudostalactites have soft cores of framboidal pyrite and show U-loops. Sulfur isotope ratios were determined in 15 samples, which result in a characteristic profile across this specimen (Table 5, Fig. 9). Colloform sphalerite/galena has $\delta^{34}S$ values decreasing in time from −1.1 to −6.9‰ (mean −3.5 ± 1.5‰). In isotopic equilibrium at low temperature, galena should be depleted in ^{34}S by about 6‰ relative to sphalerite. The absence of such a difference indicates lack of equilibrium, perhaps due to rapid crystallization. Paragenetically younger pseudostalactitic iron sulfides are much heavier with $\delta^{34}S$ 28.8 (sample enriched in framboids) to 32.9‰ (marcasite), with a mean of 31.3 ± 1.6‰. At the boundary between sphalerite and Fe sulfides, a $\delta^{34}S$ jump of 40‰ is thus documented. While our $\delta^{34}S$ values for the sphalerite and galena are in the same negative range as the values reported for stage 3 sulfides by Leach *et al.* (1996a), the isotopically heavy sulfides in our pseudostalactitic iron sulfides appear unique.

Iron isotopes and geochemistry of the Gonzen analogue site

The utility of iron isotopes for identifying biological fractionation in SFF was examined using samples from the Cady Mountains, California, and a modern mat system of the abandoned Gonzen iron mine, eastern Switzerland (Conrad, 1994; Imper, 2000; Pfeifer *et al.*, 1988). For the modern analogue, Fe-rich microbial mats were collected from a subsurface spring located ~2 km from the mine entrance. At this site, Fe-rich anoxic groundwater emerges from a flooded, inclined shaft and flows out (at ~1 liter s^{-1}) to form a small creek. Upon contact with the atmosphere, the creek waters precipitate Fe hydroxides that float on the surface of pools and coat the bottom and sides of the spring channel. Thick microbial mats that contain *Leptothrix* and *Gallionella* cover the channel walls and are heavily encrusted by Fe-(hydr)oxide precipitates (Conrad, 1994; Imper, 2000). Although no older deposits with indurated SFF fabrics were seen at this site, the perpetually dark environment and relatively constant spring flow make the site a good analogue for many SFF occurrences. Samples of water and mineral precipitates were taken at the source and 10, 22, and 31 m downstream. From the Cady Mountain site, 2 samples of Fe-encrusted filamentous fabrics and an associated calcite were analyzed (Table 6, Fig. 10). SFF samples that contain as little late-stage Fe-rich precipitate as possible were selected. Although only preliminary calcite-fluid fractionation factors have been calibrated, it is assumed that the Fe present in calcite represents the fluid without a large degree of fractionation (no redox change). Data for Gonzen samples, Fe isotopes, and trace elements are given in Table 7 and Fig. 10.

The Gonzen samples show a systematic and consistent enrichment of the heavier isotopes (0.2 and 0.5‰, respectively, as $\delta^{56}Fe$) in the precipitate over the dissolved Fe and a corresponding enrichment of ^{54}Fe in dissolved Fe downstream. Fifteen percent of dissolved Fe is precipitated over a distance of 31 m. The solid precipitates are dominated by Fe and Ca (as hydroxides and car-

Table 6. Iron Data for SFF from the Cady Mountains, California

	Cb5 SFF	*Ca18 SFF*	*Ca15*
	goethite	goethite	calcite
$\delta^{57}Fe$	0.82‰	0.61‰	−2.31
$\delta^{56}Fe$	0.57‰	0.47‰	−1.54

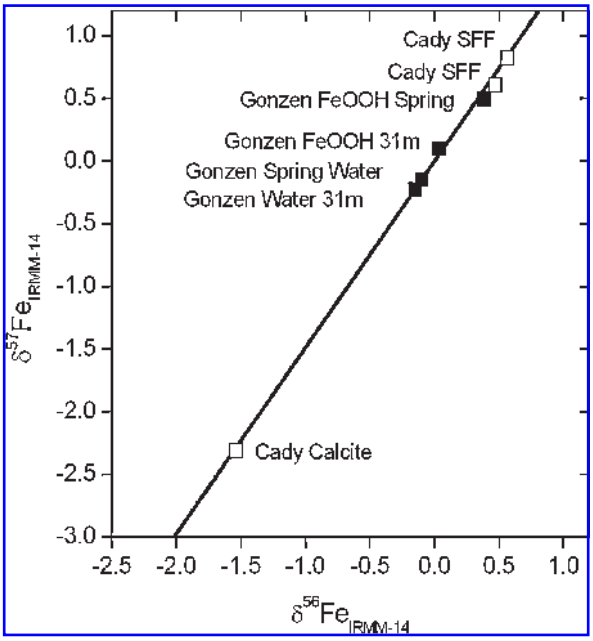

FIG. 10. Plot of Fe isotope data (δ ^{56}Fe versus δ ^{57}Fe) for solid samples from the Cady Mountains, California (Table 6), and for dissolved and suspended Fe from the Gonzen mine, Switzerland (data from Table 7). The solid line represents mass-dependent isotope fractionation. All samples lie on this line within error. Note relatively close position of Gonzen solid and dissolved iron compared with the large isotopic spread between Cady Mountains SFF (oxidized Fe) and calcite (representing dissolved Fe).

bonate), and demonstrate the coprecipitation of trace elements (As, Ba, Mo) with Fe hydroxides.

In the Cady Mountain samples, a fractionation of -2‰ (δ^{56}Fe) is observed between calcite (as proxy for the fluid composition) and isotopically heavier Fe-encrusted filaments.

DISCUSSION

Occurrences and palaeoenvironments

The environments of SFF formation can be grouped to volcanic-hosted environments, oxidized ore deposits, palaeokarst deposits, and MVT deposits, with the following characteristics: *Volcanically hosted SFF* occur in volcanics that contain primary (vesicles, lithophysae) or secondary (*e.g.*, fractures) voids that were filled entirely or partially with formation water. The timing of SFF development is difficult to constrain, but in most cases SFF formed prior to precipitation of void-filling minerals and are, therefore, thought to be early. Temperatures likely varied from ambient to the growth limits of life [now placed at ~121°C; (Kashevi and Lovley, 2003)] and increased with time due to burial in areas typically characterized by a high geothermal gradient. Conditions of pH are typically mildly alkaline (in the presence of significant hydrolysis reactions) to neutral. Energy sources include the redox potential between oxygenated near-surface water and groundwater equilibrated with host volcanic rocks. SFF that contain abundant *Gallionella*-like stalks from deposits in Breiddalur, Iceland, probably represent a regime of regional flow of groundwater that is influenced by a central volcano. *Gallionella*-like organisms may have thrived where Fe-rich waters mixed with oxygenated surface waters. Complete infilling of cavities with silica indicates a hydrothermal influence during or shortly after stalk formation. *SFF in oxidized ores* formed under near-surface conditions, possibly reaching depths of several 100 m (*e.g.*, the deep oxidation zone of the Tsumeb, Namibia ore body). Temperatures ranged from ambient to approx. 50°C due to exothermic oxidation reactions, as is indicated by stable isotope data for oxidation zone minerals from places such as Broken Hill, Australia (Melchiorre *et al.*, 2001). In such situations, sulfide oxidation releases protons that lead to acidic pH values. Potential energy sources include the oxidation of sulfide and ferrous iron. *Hydrothermal veins* that host SFF were only investigated in some detail at Menzenschwand, Germany (Hofmann, 1989; Hofmann and Eikenberg, 1991). There is evidence at the latter site for pulses of hydrothermal activity (>150°C), which results in the deposition of sulfides and quartz that is followed repeatedly by the interaction of vein material with lower-temperature more-oxidized fluids. This environment may have been conducive to the development of a community of microorganisms based on chemosynthesis. *Palaeokarst-hosted SFF* show indications of hydrothermal activity (Kretzschmar, 1982), which is supported by fluid inclusion measurements. However, the timing relative to SFF formation is unclear. As in the case of hydrothermal veins, alternating episodes of relatively low-temperature conditions favorable for microbial growth, followed by hydrothermal phases that can lead to rapid fossilization, may be invoked. Large amounts of carbonate likely buffered pH values close to slightly alkaline. In the paleokarst examples, the energy source is uncertain but could include oxidation fronts near ferrous iron-enriched sulfide or methane-rich

Table 7. Iron Isotope and Trace Element Data for a Recent Iron-Rich Spring in the Gonzen Mine, Switzerland

(A) Water from spring and associated small creek. Dissolved concentrations in ppm.

Distance from spring	*0 m*	*10 m*	*22 m*	*31 m*
T (°C)	17.4	17.4	17.2	17.1
Li	0.11	0.11	0.11	0.11
Na	40.9	40.9	40.9	39.5
Mg	26.2	26.6	26.7	26.2
Si	4.11	4.58	4.1	4.14
K	0.75	0.77	0.75	0.74
Ca	104	106	104	102
Mn	0.074	0.075	0.073	0.072
Fe	7.15	7.04	6.43	6.06
As	0.049	0.049	0.044	0.041
Sr	1.79	1.76	1.76	1.77
Mo	0.015	0.016	0.016	0.016
Ba	0.13	0.13	0.12	0.12
Fe/Mn	96.6	94.1	87.4	83.9
δ^{57}Fe dissolved	−0.15‰			−0.23‰
δ^{56}Fe dissolved	−0.10‰			−0.15‰
δ^{57}Fe suspended	0.49‰			0.10‰
δ^{56}Fe suspended	0.39‰			0.04‰

(B) Analysis of dark brown, consolidated precipitate close to Fe-rich spring. Mainly Fe hydroxide and calcite; ppm unless otherwise noted.

Na	500	As	3180
Mg	2000	Sr	985
Al	800	Mo	33
K	100	Ba	1200
Ca (%)	13.7	Sb	<0.5
Mn	384	Fe/Mn	1044
Fe (%)	40.1	As/Sb	>6300

Sampling date: August 10, 2000; air temperature at sampling site 11.8°C; pH at spring 6.6.

All water samples filtered through 0.45-micron membrane directly after collection, then acidified with ultrapure nitric acid.

seeps. *MVT-hosted SFF:* MVT deposits are typically associated with carbonate sequences along the margins of large sedimentary basins where relatively warm basinal brines mixed with cooler, fresher waters of local origin. The precipitation of sulfidic ores is thought to be at least partially related to the mixing of different groundwater masses. Such environments provide abundant chemical energy for microbial growth through redox couples such as sulfate-hydrocarbon(s) and oxygen sulfide. Temperatures may have varied from near ambient to >100°C, and pH values were probably buffered by carbonates with local excursions to acid pH values as a result of sulfide oxidation. Environments similar to those where SFF were formed likely were present at different times in the evolution of Mars or other bodies in the Solar System (Farmer, 2000).

Environments close to the surface and under influence of plant roots and soil processes (pedogenic zone) may also host structures similar to SFF. Such features have been described repeatedly as *Microcodium* (s.l.), *e.g.*, by Alonso-Zarza *et al.* (1998) and Kosir (2004). *Microcodium* may share similarities with SFF, but the relevant near-surface environment is not under consideration in this paper due to the potential influence of plants.

Morphology of SFF

The results of the analysis of filament morphology can best be explained by assuming a microbial origin for SFF. A nonbiological origin for SFF would imply that a nonbiological process formed as-yet-unobserved filaments that are different from fibrous minerals and have a width range consistently similar to that of microbial filaments. Since microbial filaments are common in

hydrothermal systems (*e.g.*, Reysenbach and Cady, 2001), while nonbiological filaments with the given characteristics are not known, the application of Occam's razor leads to the conclusion that SFF are dominantly the product of mineralization of microbial filaments. The differences observed in filament morphology between microbes collected alive and SFF may, in part, reflect the choice of species used in this study, which included forms from a broad range of environments. Observed differences may also be related to taphonomic processes due to partial degradation of filaments before fossilization by disruptive crystal growth during mineralization or other diagenetic effects. The preparation of microbial filaments collected alive on microscopic slides is another potential cause for the differences in SFF. SFF were observed in thin sections of mineral-cemented aggregates, where 3-D structures remain intact.

These data, based on the analysis of single filaments, are supported by macroscopic textures such as U-loops, which are indicative of filament flexibility. U-loops are observed in modern caves, *e.g.*, Lechuguilla, New Mexico (Boston *et al.*, 2001a). Stalactite-like features often observed in SFF have an internal microstructure (inner widths $<<$ 1mm) that is inconsistent with an origin as inorganic speleothem. Also, the spacing of vertical elements in SFF (often less than 1 mm) is much denser than in typical stalactites (typically tens of cm). Some pseudostalactites closely resemble pool fingers, a form of subaqueous, vertically draped speleothem (Adolphe *et al.*, 1991; Boston *et al.*, 2001a; Hill and Forti, 1997; Melim *et al.*, 1999). An active biologically mediated formation mechanism has been invoked for similar features observed on the wreck of the Titanic (Cullimore and Johnston, 2000), in hot springs (Tazaki *et al.*, 1998), and in caves as pool fingers (Boston *et al.*, 2001b; Hill and Forti, 1997; Melim *et al.*, 1999). Both biological and nonbiological origins have been offered for "Metallogenium" (Stein and Nealson, 1999) observed in SFF from Iceland.

Morphologies produced by nonbiological processes

As noted above, SFF show evidence that they were formed by encrustation on flexible, filamentous precursors that have widths close to 1 μm and lengths many hundreds of μm. Potential nonbiological precursors of this type could include mineral fibers, abiogenic filamentous precipitates formed within steep concentration gradients in the presence of osmotic membranes ("chemical gardens" and the like), and speleothems.

Mineral fibers: The comparison of widths of various fibrous minerals with SFF shows that SFF have a much more restricted range of widths. Also, mineral fibers have a lower curvature and show fewer directional changes. SFF precursors were flexible, as indicated by a high degree of bending and by the common presence of U-loops. SFF never show traces of mineral fibers in their core region. These arguments practically exclude mineral fibers as precursors of SFF.

Abiogenic filaments: An often-cited explanation for filamentous forms in moss agates is based on the concept of "chemical gardens" and similar experiments (Garcia-Ruiz *et al.*, 2002; Landmesser, 1984; Leduc, 1911; Liesegang, 1915; Lillie, 1917; Lillie and Johnston, 1919). In these experiments, steep chemical gradients lead to the precipitation of reaction products that act as an osmotic membrane, typically in an alkali silicate-rich medium. Such processes can produce superficially life-resembling morphologies (Leduc, 1911). More sophisticated modern experiments that use similar media can produce a range of morphologies, including twisted stalks of Ba carbonate that morphologically resemble *Gallionella* stalks (Garcia-Ruiz *et al.*, 2003). However, all these precipitates characteristically show variable widths both in filament-like forms and in twisted stalks.

Speleothems: The small width of core structures in pseudostalactitic SFF rule out a stalactitic origin where innermost core widths are in the order of 1 mm (Hill and Forti, 1997). Based on morphological similarity and occurrence in similar environments, a subaqueous origin comparable to non-stalactitic, vertically-oriented speleothems ("pool fingers") appears more likely. Actually, pool fingers are largely interpreted to be a result of microbial activity (Boston *et al.*, 2001b; Hill and Forti, 1997; Melim *et al.*, 1999) and may represent a form of SFF observed in state of formation. Helictites superficially resemble some forms of SFF but lack vertical draping and parallel organization and have larger core widths of 8–500 μm (Hill and Forti, 1997) and much larger bulk widths.

Elemental geochemistry

The geochemical data confirm that both hydrothermally influenced and palaeokarst-related SFF are Fe-rich precipitates typically with ele-

vated Fe/Mn ratios, often enriched in trace elements, most commonly As and Sb. Very similar geochemical characteristics were observed for precipitates from active Gonzen iron mine springs (Table 7), in particular the high Fe/Mn ratio, the high As concentration, and the evidence for coprecipitation of As with Fe. High trace element concentrations are interpreted as being due to adsorption on freshly precipitated Fe hydroxides, high water/solid ratios, and a high surface area. The high concentrations of trace elements observed at several sites indicate rapid element precipitation, probably at redox interfaces. The availability of redox couples at such sites is conducive to both element precipitation and microbial activity.

Sulfur isotopes

The heavy sulfur isotope values of the late-stage sulfides in the SFF sample from Poland indicate near-complete reduction of a restricted reservoir of sulphate. Similar heavy values (median 28‰) are only reported for stage 4 sulfates (Leach *et al.*, 1996a). Because stage 3 sulfides are isotopically very light, it appears likely that the pseudostalactites belong to stage 4 and are the result of near-complete reduction of a restricted reservoir of typical, isotopically heavy stage 4 sulfate. Given the low formation temperatures in the order of 50°C (Leach *et al.*, 1996a, 1996b), these data can be interpreted as the result of extensive activity of sulfate-reducing bacteria, which would generate H_2S and could lead to the near-complete reduction of local sulfate reservoirs. Alternatively, the 40‰ difference in $\delta^{34}S$ across the mineralogical interface could represent a change in sulfur source. Isotopically heavy, paragenetically late sulfides are a general feature of MVT deposits in the USA and are usually attributed to a change of sulfur redox state (Burstein *et al.*, 1993). The similarity of $\delta^{34}S$ with stage 4 sulfate and the absence of any other late-stage heavy sulfides, however, argue against such a long-distance transport of sulfide. Thus, this sample most likely represents an association of pseudostalactitic SFF and biogenic sulfate reduction. In addition, framboidal pyrite, present in this and other examples of "stalactitic" pyrite (Campbell and Barton, 1996), is considered to represent a biosignature by some authors (Popa *et al.*, 2004). At Wiesloch, Germany, the involvement of microbial sulfate reduction in the formation of sulfide ore that contains stalactite-like features has been shown by Gehlen and Nielsen (1985). At Creede, Colorado, sulfide stalactites with framboidal cores were described by Campbell and Barton (1996). Sulfur isotope studies of these features, which are likely to be related to SFF, also indicate microbial involvement in sulfide formation (Bethke *et al.*, 2000; Ilchik and Rumble, 2000). Sulfur isotopes in "stalactitic" forms made up of framboidal pyrite from cavities in fossil ammonites (Hudson, 1982) also indicate concomitant microbial activity and "stalactite" formation. Based on our example, these literature data, which consist of at least 5 examples of "stalactitic" sulfides that are morphologically related to SFF, show sulfur isotopic evidence of growth in association with microbial sulfate reduction.

Iron isotopes

It has been suggested that Fe isotopes may be used to identify the chemical signature of microbial metabolism (Beard and Johnson, 1999). Recent work, however, has shown that abiogenic isotope fractionations that are mostly related to redox processes (Bullen *et al.*, 2001; Johnson *et al.*, 2002; Markl *et al.*, 2006) are approximately twice as large as those produced by dissimilatory Fe-reducing bacteria or by Fe-oxidizing phototrophs (Beard *et al.*, 2003; Johnson *et al.*, 2005).

The Fe isotope composition of each of the 2 dissolved Gonzen samples is indistinguishable within the measurement error. The fractionation of 0.2 and 0.5‰ between water and solid of $\delta^{56}Fe$ is of the same sense (solid enriched in the heavier isotope), but smaller than that observed in several abiogenic experiments (Bullen *et al.*, 2001; Johnson *et al.*, 2005) and at sites of abiogenic natural precipitation (Bullen *et al.*, 2001). Apparently, in the Gonzen mine spring, biological Fe oxidation produces no Fe isotope fractionation significantly larger than that observed during abiogenic precipitation. This is in line with experimental calibration of microbial Fe metabolism, which appears to result in smaller Fe isotope fractionation than is observed during abiogenic reactions (Brantley *et al.*, 2001; Johnson *et al.*, 2005).

In the Cady Mountain samples, a fractionation of 2‰ ($\delta^{56}Fe$) is observed between calcite and Fe-encrusted filaments. This value is relatively large compared with other studies (Yamaguchi *et al.*, 2005, Markl *et al.*, 2006), but is still in the range of observed abiogenic fractionations. The relative

position of the samples and strong depletion of calcite in the heavy isotopes is in accordance with massive oxidative Fe precipitation (organic or inorganic) in this system. We can say this because oxidation of dissolved ferrous Fe is associated with a +3‰ fractionation in δ^{56}Fe (Welch *et al.*, 2003), while FeOOH precipitation from dissolved ferric Fe potentially entails a reverse fractionation of −1.5‰. This results in a net enrichment of *ca.* +1.5‰ in the ferric precipitate as was observed in natural stream settings (Bullen *et al.*, 2001). In contrast, carbonate precipitation from dissolved ferrous Fe results in only small fractionations (reviewed by Yamaguchi *et al.*, 2005). Therefore the Cady Mountain calcite composition serves as a proxy for the fluid composition.

To date, no conclusive evidence exists that would suggest that these fractionations are characteristic of biotic processes. Fractionation during goethite and hematite reduction by dissimilatory iron-reducing bacteria resulted in a ferrous fluid that was −3‰ reduced in δ^{56}Fe (Crosby *et al.*, 2005), while oxidation of dissolved ferrous Fe by photoautotrophic bacteria results in a fractionation of +1.5‰ for the oxidized species (Croal *et al.*, 2004). Our observations encompass these fractionations, but they are not significantly different from abiotic effects.

Biogenic versus abiogenic origin of SFF

Examples of filamentous fabrics formed at the sea surface in hot-spring environments have been described in numerous examples of active and fossil sites (Duhig *et al.*, 1992; Iizasa *et al.*, 1998; Ishizuka and Imai, 1998; Juniper and Fouquet, 1988; Juniper *et al.*, 1995; Juniper and Sarrazin, 1995; Little *et al.*, 1999; Pracejus and Halbach, 1996; Rasmussen, 2000; Zierenberg and Schiffman, 1990). All these occurrences have previously been interpreted as having a biological origin. An abiogenic origin was advocated for similar structures (referred to as moss agate) from the TAG site by Hopkinson *et al.* (1998). Several occurrences of SFF described in recent years (Baele, 1999; Feldmann *et al.*, 1997; Geptner *et al.*, 2004; Kretzschmar, 1982; Schumann *et al.*, 2004; Trewin and Knoll, 1999) were interpreted as having a biological origin, as was the case in a previously published general paper on SFF (Hofmann and Farmer, 2000). Previous biological interpretations cited above were based primarily on filamentous morphology. More recently, reliance on such morphological arguments for evaluating biogenicity has been heavily criticized by some authors (Garcia-Ruiz, 1994, 2001; Garcia-Ruiz and Amoros, 1998; Garcia-Ruiz *et al.*, 2002) based on experimental evidence that similar features can be produced in the laboratory by abiogenic processes.

In the present study, we have attempted to integrate multiple lines of morphological, microstructural, geochemical, and mineralogical evidence to better constrain the nature of environments where SFF were formed and to use this as a starting point for evaluating biological hypotheses. A fundamental feature of all the SFF we have studied is the presence of a cylindrical core region of nearly constant, small (~1.0 μm) width that served as a site for the initial nucleation of precipitating minerals. This filamentous core provided a template that controlled the pattern of subsequent precipitation and produced the mesoscale fabrics observed in SFF. Our morphometric analysis suggests that this core was comprised of highly flexible filaments that were later removed, which left a central mold that was then infilled by later mineral phases. This pattern is typical of what is observed during microbial fossilization processes in a wide variety of modern mineralizing surface systems (Cady and Farmer, 1996; Farmer, 1999a).

In oxidizing systems where organic materials were present, these were almost always lost during early diagenesis. However, we demonstrate that a detailed morphometric analysis of even the simple filamentous forms left behind can be quite informative and that some parameters (those sensitive to curvature and tortuosity) appear to be particularly useful for discriminating biological and nonbiological materials. Furthermore, the sensitivity of these parameters and their utility for discriminating between biology and an abiogenic origin can be easily explained in terms of the inherent properties of biological materials and microbial taxis.

Summary of arguments favoring a biogenic origin of most SFF samples

With regard to several localities investigated, independent arguments for the activity of microbes during the formation of filamentous fabrics have been made. Isotopic evidence for biogenic carbon oxidation based on light carbon in pseudostalactite-associated calcite is present at

Agrigento, Sicily (Dessau *et al.*, 1962). Similar evidence exists at Broken Hill, Australia, in the form of light C isotopes in cerussite (Melchiorre and Williams, 2001) present in SFF-dominated gossan material as observed in this study.

A number of arguments thus render several abiogenic explanations unlikely for the majority of SFF:

- The steep concentration and pH gradients necessary for the formation of abiogenic filaments in the sense of Garcia-Ruiz *et al.* (2003) are rarely found in natural environments. Environments where such gradients are present (*e.g.*, hot and cold vents) are not typically hosts for SFF.
- All forms of abiogenic filaments are formed in an alkaline medium rich in dissolved silica. Geological evidence indicates that morphologically similar SFF were formed in various types of environments, some of which may have been silica rich and high pH (volcanic host rocks), while others (*e.g.*, oxidizing sulfide deposits) were low pH.
- Abiogenic filaments formed experimentally (Garcia-Ruiz *et al.*, 2003) have been produced from a viscous, partly colloidal medium (alkali silicate). Most examples of SFF clearly lack evidence for growth within a colloidal matrix. The removal of such a matrix by flowing water would most likely have destroyed delicate abiogenic filaments. SFF filaments, rather, formed as encrustations of filaments growing in a water-filled void, as is often indicated by vertical orientation of filaments. Where an enclosing medium was present, it is clearly a secondary infill that postdates the formation of the filaments, *e.g.*, where filamentous fabrics partly stick out of layered ("Uruguay-type") agate. There are examples where morphologically similar SFF were later enclosed by different minerals (*e.g.*, Cady Mountains, California, by chalcedony and calcite), which demonstrates that the SFF are independent of later cementation.
- SFF from chemically and geologically diverse environments have core widths close to 1 μm with a narrow distribution of values. The width of abiogenic filaments is dependent on the chemical conditions and can be expected to show a wide range of values.

Characteristics of SFF, many of them indicating an involvement of microbes, are summarized in Table 8.

Geochemical analyses demonstrate that, not surprisingly, trace element concentrations are highly variable in subsurface precipitates that contain filamentous fabrics. However, As and Sb are most systematically enriched together with Fe and Mn, with minor Mo, V, W, U, while immobile elements are depleted due to dilution by mineral precipitates. It appears most likely that these elements were concentrated mainly by adsorption on Fe hydroxides. As and Sb are relatively mobile elements both under near-surface weathering conditions and in low-temperature hydrothermal solutions. In general, the geochemistry of SFF is indicative of a water-rich environment under oxidizing conditions, which favors precipitation of Fe-Mn-hydroxides and is conducive to the sequestration of trace elements.

Events leading to the formation of SFF

Presently, we can only speculate about the details of SFF genesis. The presence of large numbers of filaments that were rapidly mineralized appears at first glance hardly compatible with a very low growth rate that would be typical for many steady-state subsurface environments (Chapelle *et al.*, 2002; D'Hondt *et al.*, 2002; Weiss *et al.*, 2000). However, considering the apparent flow-through nature of most SFF-containing systems and the presence of steep redox gradients constantly renewed by flow, relatively high biomass could accumulate over extended periods of time. Additionally, in rapidly mineralizing environments, microbes must avoid becoming incorporated into the precipitation front. With the potential for motility, even under conditions of slow precipitation and microbial growth, it appears likely that a substantial SFF deposit could build up over a fairly short period of time. Episodic periods of enhanced microbial growth could also be induced by seismic events, rapid sulfide oxidation, or other geological processes that could release larger amounts of chemical energy. Rapid mineralization favorable for microtextural (biofabric) preservation, then, may also be a result of the same dynamic geological environment. Filamentous morphologies would enhance the surface area of microbial colonies in a rock void of a given volume because 3-dimensional, rather than

Table 8. Comparison of Filament Characteristics

Characteristics considered typical for biogenic origin	*SFF*
Median width of filaments <5 μm with narrow, near-normal distributions of low skewness	common
Single filaments show ~constant thickness over their length	common
Filaments show high degrees of bending (median >0.5°/μm)	common
Evidence of flexibility (bending) prior to mineral encrustation (U-loops)	common
Filaments show many direction changes along length (median >10/mm)	common
Close association of SFF and *Gallionella*-like morphologies	observed at 2 sites
Presence of matted fabrics	common
Formation of rope-like (braided) fabrics	several occurrences
Vertically oriented sheets of closely spaced, ~parallel filaments (<1 cm)	common
Filaments with core regions having a width <<1 mm	common
Low temperature (<100°C) host mineral assemblage	all cases
Geometry of fabric independent of mineralogy/milieu	common
Isotopic evidence for presence of microbes during formation	several occurrences
Characteristics considered typical for abiogenic origin	
Evidence of mineral fibers	rare
Radial orientation of filaments/fibers	not observed

surficial, colonization is facilitated and promotes nutrient uptake within the volume-restricted environment of a subsurface fracture. This may explain the dominance of filamentous fabrics in the SFF associations we describe here.

A microbial bloom is only possible if suitable sources of nutrients are available. One critical element may be phosphorous, which tends to adsorb onto iron hydroxides (Bjerrum and Canfield, 2002). Evidence for phases of P mobilization is present in oxidized ore bodies, where the occurrence of large amounts of phosphate minerals (*e.g.*, pyromorphite) indicates episodic high P concentrations, possibly as a result of Fe-hydroxide dissolution or biomass degradation.

Relevance for the search for life on Mars

SFF are characteristic and widespread features in terrestrial rocks that show low-temperature hydrothermal and oxidative alteration. As similar situations are likely to have been common on Mars (Farmer, 1999b), it follows that, if life ever developed in subsurface environments on Mars (indeed, the subsurface remains the most likely long-term habitat for martian life), then SFF might also be expected to be present in a range of subsurface hydrothermal deposits. Thus, in the context of Mars exploration, an understanding of SFF genesis appears highly relevant for astrobiology. The characteristic meso- and microscale features of SFF lend themselves well to rover-based visualization tools and should be considered viable exploration targets during upcoming landed missions. SFF do exclude, by definition, any fabrics made up by nonfilamentous microbes. Our focus on filamentous forms appears justified because (A) filamentous microbes are known to be present in the Archean (Rasmussen, 2000; Walsh and Lowe, 1985; Walsh and Westall, 2003; Westall *et al.*, 2006) and, therefore, represent an early development of life; (B) filaments are more characteristic than coccoid shapes, even after massive encrustation by minerals, and are more easily recognized; (C) filaments may biologically arise from filamentous microbes but also from mineralized microbial exopolymers (Jones *et al.*, 2004; Westall *et al.*, 2000); (D) the morphology of nonbiological filaments is distinct from biological ones.

This study demonstrates that non-sedimentary host rock lithologies, such as volcanics and impactites, are important targets for astrobiology because of their potential to harbor aqueous precipitates at a variety of observational scales. Possible host lithologies on Mars include vesicular and fractured volcanics, impactites, oxidized sulfide-rich rocks, and porous sediments. Energy sources may have been derived from the oxidation of sulfide, ferrous Fe, or hydrogen. Relatively oxidizing environments would be required to provide the necessary redox potential. Such oxidizing conditions are suggested by the presence of abundant hematite concretions in sediments at

Meridiani Planum as observed by the Mars Exploration Rover Opportunity (Chan *et al.*, 2005; Knoll *et al.*, 2005; Squyres *et al.*, 2004). Even though martian background levels of As and Sb (typically enriched in terrestrial SFF) are probably lower than on Earth (Lodders, 1998), these elements may be useful indicators of aqueous Fe-hydroxide precipitation.

CONCLUSIONS

SFF are very widespread in several terrestrial subsurface environments. Despite the variability of host environments, the morphology of SFF is very similar across the range of environmental circumstances. Organic preservation of microbial filaments is rare in generally oxidizing environments. However, studies of microbial fossilization processes in modern hydrothermal systems have revealed taphonomic processes and end products comparable to the patterns observed in SFF. Such comparisons suggest that the majority of SFF are likely to have been formed by mineral encrustation of biogenic filaments. A number of criteria, most prominently filament width, bending, and number of direction changes in filaments, show that most SFF are more closely related to microbial filaments than to abiogenic mineral fibers. The high density of filaments in many occurrences along with evidence of rapid subsequent mineral precipitation indicate that SFF were formed at sites with a high availability of chemical energy. It is anticipated that a better understanding of SFF formation will result from future investigations of their *in situ* formation in subsurface mines or wells using field-deployed experiments. Certain SFF may also have formed from encrustation of mineral fibers in cavities. Macroscopic SFF are thus considered not as proof, but as an indicator, of an involvement of microbes in their formation. Further evidence can then be obtained using microtextural and geochemical arguments.

Similar conditions as those that led to the formation of SFF were likely present on Mars earlier in the evolution of that planet, and may have developed anywhere in the Solar System where hydrothermal habitats supported filamentous microbial life-forms. As the fossil record of subsurface microbial ecosystems, biogenic SFF represent an important exploration target for Mars exopaleontology.

ACKNOWLEDGMENTS

Research leading to this paper has been supported by a grant by Entwicklungsfonds Seltene Metalle, Pully (Switzerland) to B.A.H. and grants from NASA's Exobiology Program and the NASA Astrobiology Institute to J.D.F. We thank Ph. Häuselmann for support with the SEM and help in the field and cave discussions. Thanks to all those who helped with locating SFF samples: P. Andersen, J. Arnoth, F. Betschart, H. Gamma, and P. and G. Penkert. K. Hanselmann, F. Schenker, and W. Eugster initiated, supported, and allowed the Gonzen fieldwork. Thanks to H. Baur for help with multivariate statistics. Constructive comments of two anonymous reviewers greatly improved the manuscript.

ABBREVIATONS

INAA, Instrumental neutron activation analysis; MVT, Mississippi Valley–Type base-metal deposits; NMBE, Natural History Museum Bern; SFF, subsurface filamentous fabrics; SEM, scanning electron microscopy.

REFERENCES

Adolphe, J.-P., Choppy, B., Loubière, J.-F., Paradas, J., and Loleilhavoup, F. (1991) Biologie et concretionnement: un exemple, les baguettes de gours. *Karstologia* 18, 49–55.

Alonso-Zarza, A.M., Sanz, M.E., Calvo, J.P., and Estévez, P. (1998) Calcified root cells in Miocene pedogenic carbonates of the Madrid Basin: evidence for the origin of *Microcodium*. *Sediment. Geol.* 16, 81–97.

Amy, P.S. and Haldeman, D.L. (1997) *The Microbiology of the Terrestrial Deep Subsurface*, Lewis, Boca Raton.

Audra, P. and Hofmann, B.A. (2004) Les cavités hypogènes associées aux dépôts de sulfures métalliques (MVT). *Le Grotte d'Italia* 5, 35–56.

Baele, J.-M. (1999) Karst and silification in continental and margino-littoral environment: two examples in the Meso-Cenozoic of Southern Belgium. In *Karst 99,* edited by P. Audra, Université de Provence, Grands Causses, Vercors, France, pp. 49–54.

Banfield, J.F., Welch, S.A., Zhang, H., Ebert, T.T., and Penn, R.L. (2000) Aggregation-based crystal growth and microstructure development in natural iron oxyhydroxide biomineralization products. *Science* 289, 751–754.

Beard, B.L. and Johnson, C.M. (1999) High precision iron isotope measurements of terrestrial and lunar materials. *Geochim. Cosmochim. Acta* 63, 1653–1660.

Beard, B.L., Johnson, C.M., Skulan, J.L., Nealson, K.H., Cox, L., and Sun, H. (2003) Application of Fe isotopes to tracing the geochemical and biological cycling of Fe. *Chem. Geol.* 195, 87–117.

Bethke, P.M., Rye, R.O., and Finkelstein, D.B. (2000) Isotopic studies of authigenetic sulfides, silicates, and carbonates, and calcite and pyrite veinlets in the Creede Formation, San Juan Mountains, southwestern Colorado. In *Ancient Lake Creede, Geologial Society of America Special Paper 346,* edited by P.M. Bethke and R.L. Hay, pp. 267–286.

Bjerrum, C.J. and Canfield, D.E. (2002) Ocean productivity before about 1.9 Gyr ago limited by phosphorus adsorption onto iron oxides. *Nature* 417, 159–162.

Boston, P.J., Spilde, M.N., Northup, D.E., and Melim, L.A. (2001a) Cave microbe-mineral suites: best model for extraterrestrial biosignatures [abstract 2015]. In *32nd Lunar and Planetary Science Conference,* Lunar and Planetary Institute, Houston.

Boston, P.J., Spilde, M.N., Northup, D.E., Melim, L.A., Soroka, D.S., Kleina, L.G., Lavoie, K.H., Hose, L.D., Mallory, L.M., Dahm, C.N., Crossey, L.J., and Schelble, R.T. (2001b) Cave biosignature suites: microbes, minerals, and Mars. *Astrobiology* 1, 25–55.

Bowerbank, J.S. (1842) On the spongeous origin of moss agates and other siliceous bodies. *Annals and Magazine of Natural History* 10, 9–18, 84–91.

Brantley, S.L., Liermann, L., and Bullen, T.D. (2001) Fractionation of Fe isotopes by soil microbes and organic acids. *Geology* 29, 535–538.

Brasier, M.D., Green, O.R., Jephcoat, A.P., Kleppe, A.K., Van Kranendonk, M.J., Lindsay, J.F., Steele, A., and Grassineau, N.V. (2002) Questioning the evidence for Earth's oldest fossils. *Nature* 416, 76–81.

Braun, A. and Wilde, V. (2001) Systematik und Erhaltung eines Restes von Kalymma (Calamopityaceae) aus dem Unterkarbon des Kellerwaldes (Hessen, Deutschland). *Senckenbergiana lethaea* 81, 263–281.

Brown, R.W. (1957) Plantlike features in thunder eggs and geodes. In *Annual Report of the Board of Regents of the Smithsonian Institution,* Smithsonian Institution, Washington, DC, pp. 329–339.

Bullen, T.D., White, A.F., Childs, C.W., Vivit, D.V., and Schulz, M.S. (2001) Demonstration of significant abiotic iron isotope fractionation in nature. *Geology* 29, 699–702.

Burstein, I.B., Shelton, K.L., Gregg, J.M., and Hagni, R.D. (1993) Complex, multiple ore-fluids in the world-class Southeast Missouri Pb-Zn-Cu deposits: sulfur isotope evidence. In *Geology and Geochemistry of Mississippi Valley-Type Ore Deposits*, edited by K.L. Shelton and R.D. Hagni, University of Missouri-Rolla, Rolla, Missouri, pp. 1–15.

Buseck, P.R., Dunin-Borkowski, R.E., Devouard, B., Frankel, R.B., McCartney, M.R., Midgley, P.A., Posfai, M., and Weyland, M. (2001) Magnetite morphology and life on Mars. *Proc. Natl. Acad. Sci. U.S.A.* 98, 13490–13495.

Cady, S.L. and Farmer, J.D. (1996) Fossilization processes in silicous thermal springs: trends in preservation along thermal gradients. In *Evolution of Hydrothermal Ecosystems on Earth (and Mars?), Ciba Foundation Symposium 202,* edited by G.R. Bock and J.A. Goode, John Wiley and Sons, Chichester, UK, pp. 150–173.

Cady, S.L., Farmer, J.D., Grotzinger, J.P., Schopf, J.W., and Steele, A. (2003) Morphological biosignatures and the search for life on Mars. *Astrobiology* 3, 351–368.

Campbell, W.R. and Barton, P.B. (1996) Occurrence and significance of stalactites within the epithermal deposits at Creede, Colorado. *Can. Mineral.* 34, 905–930.

Chan, M.A., Beitler Bowen, B., Parry, W.T., Ormö, J., and Komatsu, G. (2005) Red rock and red planet diagenesis: comparisons of Earth and Mars concretions. *GSA Today* 15, 4–10.

Chapelle, F.H., O'Neill, K., Bradley, P.M., Methé, B.A., Ciufo, S.A., Knobel, L.L., and Lovley, D.R. (2002) A hydrogen-based subsurface microbial community dominated by methanogens. *Nature* 415, 312–315.

Conrad, H. (1994) Die kleinsten Bergmännchen der Welt—von Sargans bis Barberton. *Terra Plana* 2/94, 23–30.

Croal, L.R., Johnson, C.M., Beard, B.L., and Newman, D.K., (2004) Iron isotope fractionation by Fe(II)-oxidizing photoautotrophic bacteria. *Geochim. Cosmochim. Acta* 68, 1227–1242.

Crosby, H.A., Johnson, C.M., Roden, E.E., and Beard, B.L. (2005) Coupled Fe(II)-Fe(III) electron and atom exchange as a mechanism for Fe isotope fractionation during dissimilatory iron oxide reduction. *Environ. Sci. Technol.* 39, 6698–6704.

Cullimore, D.R. and Johnston, L. (2000) Biodeterioration of the RMS Titanic. *Canadian Chemical News* Nov/Dec. 2000, 14–15.

Cunningham, K.I., Duchene, H.R., McLean, J.S., and Spirakis, C.S. (1994a) Terrestrial hypogenic caves: possible analogs to subterranean martian autotrophic ecosystems. In *Breakthroughs in Karst Geomicrobiology and Redox Chemistry,* edited by I.D. Sasowsky and M.V. Palmer, Karst Waters Institute, Colorado Springs, pp. 12–13.

Cunningham, K.I., Northup, D.E., Pollastro, R.M., Wright, W.G., and Larock, E.J. (1994b) Bacterial and fungal habitation in Lechuguilla cave, Carlsbad Caverns National Park, New Mexico—possible biologic origin of condensation-corrosion residues. In *Breakthroughs in Karst Geomicrobiology and Redox Chemistry,* edited by I.D. Sasowsky and M.V. Palmer, Karst Waters Institute, Colorado Springs, pp. 13–14.

Daubenton, L.J.M. (1782) Sur les causes qui produisent trois sortes d'herborisations dans les pierres. *Mémoires de l'Académie Royale des Sciences* 1782, 667–673.

Dessau, G., Jensen, M.L., and Nakai, N. (1962) Geology and isotopic studies of Sicilian sulfur deposits. *Econ. Geol.* 57, 410–438.

Dexter-Dyer, B., Kretzschmar, M., and Krumbein, W.E. (1984) Possible microbial pathways in the formation of Precambrian ore deposits. *J. Geol. Soc. London* 141, 251–262.

D'Hondt, S., Rutherford, S., and Spivack, A.J. (2002) Metabolic activity of subsurface life in deep-sea sediments. *Science* 295, 2067–2070.

D'Hondt S., Jørgensen, B.B., Miller, J., Batzke, A., Blake, R., Cragg, B.A., Cypionka, H., Dickens, G.R., Ferdelman, T., Hinrichs, K.-U., Holm, N.G., Mitterer, R., Spivack, A., Wang, G., Bekins, B., Engelen, B., Ford, K., Gettemy, G., Rutherford, S.D., Sass, H., Skilbeck, C.G., Aiello, I.W., Guèrin, G., House, C.H., Inagaki, F., Meister, P., Naehr, T., Niitsuma, S., Parkes, R.J., Schippers, A., Smith, D.C., Teske, A., Wiegel, J., Naranjo Padilla, C., and Solis Acosta, J.L. (2004) Distributions of microbial activities in deep subseafloor sediments. *Science* 306, 2216–2221.

Diakonov, I., Khodakovsky, I., Schott, J., and Sergeeva, E. (1994) Thermodynamic properties of iron oxides and hydroxides. I. Surface and bulk thermodynamic properties of goethite (α-FeOOH) up to 500 K. *European Journal of Mineralogy* 6, 967–983.

Dubinina, G.A. (1970) Untersuchungen über die Morphologie von Metallogenium und die Beziehungen zu Mycoplasma. *Zeitschrift für allgemeine Mikrobiologie* 10, 309–320.

Duhig, N.C., Davidson, G.J., and Stolz, J. (1992) Microbial involvement in the formation of Cambrian sea-floor silica-iron oxide deposits, Australia. *Geology* 20, 511–514.

Edwards, K.J., Bond, P.L., Druschel, G.K., McGuire, M.M., Hamers, R.J., and Banfield, J.F. (2000) Geochemical and biological aspects of sulfide mineral dissolution: lessons from Iron Mountain, California. *Chem. Geol.* 169, 282–297.

Ellis D. (1919) *Iron Bacteria*, Methuen & Co. Ltd., London.

Farmer, J. (1999a) Taphonomic modes in microbial fossilization. In *Workshop on Size Limits of Very Small Microorganisms: Proceedings of a Workshop*, edited by S.G.O., Space Studies Board, National Research Council, National Academy Press, Washington DC, pp. 94–102.

Farmer, J.D. (1999b) Implementing a strategy to explore for ancient martian life. In *The Search for Life on Mars*, edited by J.A. Hiscox, British Interplanetary Society, London, pp. 58–65.

Farmer, J.D. (2000) Hydrothermal systems: doorways to early biosphere evolution. *GSA Today* 10, 1–9.

Feldmann, M., Neher, J., Jung, W., and Graf, F. (1997) Fungal quartz weathering and iron crystallite formation in an alpine environment, Piz Alv, Switzerland. *Eclogae Geologicae Helvetiae* 90, 541–556.

Ferris, F.G., Konhauser, K.O., Lyvén, B., and Pedersen, K. (1999) Accumulation of metals by bacteriogenic iron oxides in a subterranean environment. *Geomicrobiol. J.* 16, 181–192.

Feucht, C. (2006) Geologie, Sekundärmineralien und Biosignaturen tertiärer Basalte, Breiddalur, Ostisland. Masters thesis, Universität Bern, Bern.

Feucht, C., Hüsser, B., and Hofmann, B.A. (2006) Fossil *Gallionella* microbes in ancient subsurface habitats from Tertiary basalts of eastern Iceland. In *5th European Workshop on Astrobiology, Budapest, Oct. 2005. Int. J. Astrobiology* 5/1(86).

Fisk, M.R., Giovannoni, S.J., and Thorset, I.H. (1998) Alteration of oceanic volcanic glass: textural evidence of microbial activity. *Science* 281, 978–980.

Fisk, M.R., Popa, R., Mason, O.U., Storrie-Lombardi, M.C., and Vicenzi, E.P. (2006) Iron-magnesium silicate bioweathering on Earth (and Mars?). *Astrobiology* 6, 48–68.

Friedman, E.I., Wierzchos, J., Ascaso, C., and Winklhofer, M. (2001) Chains of magnetite crystals in the meteorite ALH84001: evidence of biological origin. *Proc. Natl. Acad. Sci. U.S.A.* 98, 2176–2181.

Garcia-Ruiz, J.M. (1994) Inorganic self-organization in Precambrian cherts. *Orig. Life Evol. Biosph.* 24, 451–467.

Garcia-Ruiz, J.M. (2001) Morphological behaviour of inorganic precipitation systems and primitive life detection. In *Crystallogenesis and Mineralogy*, Saint Petersburg, Russia, pp. 119.

Garcia-Ruiz, J.M. and Amoros, J.L. (1998) Carbonate precipitation into alkaline silica-rich environments. *Geology* 26, 843–846.

Garcia-Ruiz, J.M., Carnerup, A., Christy, A.G., Welham, N.J., and Hyde, S.T. (2002) Morphology: an ambigous indicator of biogenicity. *Astrobiology* 2, 335–351.

Garcia-Ruiz, J.M., Hyde, S.T., Carnerup, A.M., Christy, A.G., Van Kranendonk, M.J., and Welham, N.J. (2003) Self-assembled silica-carbonate structures and detection of ancient microfossils. *Science* 302, 1194–1197.

Gehlen, K.V. and Nielsen, H. (1985) Extreme sulphur isotope fractionation in Zn-Pb ores at Wiesloch, FRG. *Terra Cognita* 5, 154–155.

Geptner, A., Kristmannsdottir, H., and Pikovskii, Y. (2004) Mineralized microbiota as an indicator of hydrocarbon upflows in modern and ancient time in Iceland. *Astrobiology* 4, 253–254.

Ghiorse, W.C. (1997) Subterranean life. *Science* 275, 789–790.

Gold, T. (1992) The deep, hot biosphere. *Proc. Natl. Acad. Sci. U.S.A.* 89, 6045–6049.

Gold, T. (1999) *The Deep Hot Biosphere*, Copernicus, New York.

Hallbeck, L. and Pedersen, K. (1995) Benefits associated with the stalk of *Gallionella ferruginea*, evaluated by comparison of a stalk-forming and a non-stalk-forming strain and biofilm studies *in situ*. *Microb. Ecol.* 30, 257–268.

Hallbeck, L., Ståhl, F., and Pedersen, K. (1993) Phylogeny and phenotypic characterization of the stalk-forming and iron-oxidizing bacterium *Gallionella ferruginea*. *J. Gen. Microbiol.* 139, 1531–1535.

Hallberg, K.B., Coupland, K., Kimura, S., and Johnson, D.B. (2006) macroscopic streamer growths in acidic, metal-rich mine waters in north Wales consist of novel and remarkably simple bacterial communities. *Appl. Environ. Microbiol.* 72, 2022–2030.

Hill, C. and Forti, P. (1997) *Cave Minerals of the World*, National Speleological Society, Huntsville, Alabama.

Hofmann B. (1989) Genese, Alteration und rezentes Fliess-System der Uranlagerstätte Krunkelbach (Menzenschwand, Südschwarzwald). Nagra, Baden.

Hofmann, B. and Eikenberg, J. (1991) The Krunkelbach uranium deposit, Schwarzwald, Germany: correlation of radiometric ages (U-Pb, U-Xe-Kr, K-Ar, ^{230}Th-^{234}U)

with mineralogical stages and fluid inclusions. *Econ. Geol.* 86, 1031–1049.

Hofmann, B.A. and Farmer, J.D. (2000) Filamentous fabrics in low-temperature mineral assemblages: are they fossil biomarkers? Implications for the search for a subsurface fossil record on the early Earth and Mars. *Planet. Space Sci.* 48, 1077–1086.

Hopkinson, L., Roberts, S., Herrington, R., and Wilkinson, J. (1998) Self-organization of submarine hydrothermal siliceous deposits: evidence from the TAG hydrothermal mound, 26°N Mid-Atlantic Ridge. *Geology* 26, 347–350.

Hudson, J.D. (1982) Pyrite in ammonite-bearing shales from the Jurassic of England and Germany. *Sedimentology* 29, 639–667.

Iizasa, K., Kawasaki, K., Maeda, K., Matsumoto, T., Saito, N., and Hirai, K. (1998) Hydrothermal sulfide-bearing Fe-Si oxyhydroxide deposits from the Coriolis Troughs, Vanuatu backarc, southwestern Pacific. *Mar. Geol.* 145, 1–21.

Ilchik, R.P. and Rumble, D.R., III. (2000) Sulfur, carbon and oxygen isotope geochemistry of pyrite and calcite from veins and sediment samples by borehole CCM-2, Creede Caldera, Colorado. In *Ancient Lake Creede, Geologial Society of America Special Paper 346,* edited by P.M. Bethke and R.L. Hay, pp. 287–300.

Imper, D. (2000) Bergwasser- und Grubengasuntersuchungen im Eisenbergwerk Gonzen (Sargans und Wartau SG). *Berichte der St.Gallischen Naturwiss. Ges.* 89, 57–78.

Ishizuka, O. and Imai, A. (1998) "Brown Ore" from the Fukasawa Kuroko Deposit, northeast Japan: its characteristics and formation process. *Resource Geology* 48, 53–73.

Johnson, C.M., Skulan, J.L., Beard, B.L., Sun, H., Nealson, K.H., and Braterman, P.S. (2002) Isotopic fractionation between Fe(III) and Fe(II) in aqueous solutions. *Earth Planet. Sci. Lett.* 195, 141–153.

Johnson, C.M., Beard, B.L., Welch, S.A., Roden, E.E., Croal, L.R., Newman, D.K., and Nealson, K.H. (2005) Experimental constraints on Fe isotope fractionations during magnetite and Fe carbonate formation coupled to dissimilatory hydrous ferric oxide reduction. *Geochim. Cosmochim. Acta* 69, 963–993.

Jones, B., Konhauser, K.O., Renaut, R.W., and Wheeler, R.S. (2004) Microbial silicification in Iodine Pool, Waimangu geothermal area, North Island, New Zealand: implications for recognition and identification of ancient silicified microbes. *J. Geol. Soc. London* 161, 983–993.

Juniper, S.K. and Fouquet, Y. (1988) Filamentous iron-silica deposits from modern and ancient hydrothermal sites. *Can. Mineral.* 26, 859–869.

Juniper, S.K. and Sarrazin, J. (1995) Interaction of vent biota and hydrothermal deposits: present evidence and future experimentation. In *Seafloor Hydrothermal Systems,* edited by S.E. Humphris, R.A. Zierenberg, L.S. Mullineaux, and R.E. Thomson, American Geophysical Union, Washington, DC, pp. 178–193.

Juniper, S.K., Martineu, P., Sarrazin, J., and Gélinas, Y. (1995) Microbial-mineral floc associated with nascent hydrothermal activity on CoAxial Segment, Juan de Fuca Ridge. *Geophys. Res. Lett.* 22, 179–182.

Kashevi, K. and Lovley, D.R. (2003) Extending the upper temperature limit for life. *Science* 301, 934.

Klaveness, D. (1977) Morphology, distribution and significance of the manganese-accumulating microorganism metallogenium in lakes. *Hydrobiologia* 56, 25–33.

Knoll, A.H., Carr, M., Clark, B., Des Marais, D.J., Farmer, J.D., Fischer, W.W., Grotzinger, J.P., McLennan, S.M., Malin, M., Schröder, C., Squyres, S., Tosca, N.J., and Wdowiak, T. (2005) An astrobiological perspective on Meridiani Planum. *Earth Planet. Sci. Lett.* 240, 179–189.

Kosir, A. (2004) Microcodium revisited: root calcification products of terrestrial plants on carbonate-rich substrates. *J. Sediment. Res.* 74, 845–857.

Kretzschmar, M. (1982) Fossile Pilze in Eisen-Stromatolithen von Warstein (Rheinisches Schiefergebirge). *Facies* 7, 237–260.

Krumholz, L.R., McKinley, J.P., Ulrich, G.A., and Suflita, J.M. (1997) Confined subsurface microbial communities in Cretaceous rock. *Nature* 386, 64–66.

Landmesser, M. (1984) Das Problem der Achatgenese. *Pollichia* 72, 5–137.

Leach, D.L., Viets, J.G., and Gent, C.A. (1996a) Sulfur isotope geochemistry of ore and gangue minerals from the Silesia-Cracow Mississippi Valley–type ore district, Poland. *Prace Panstwowego Instytutu Geologicznego* 154, 123–137.

Leach, D.L., Viets, J.G., and Powell, J.W. (1996b) Textures of ores from the Silesian-Cracow zinc-lead deposits, Poland: clues to the ore-forming environment. *Prace Panstwowego Instytutu Geologicznego* 154, 37–51.

Leduc, S. (1911) *The Mechanisms of Life*, Rebman, London.

Lieber, W. (2001) Stalaktiten im Mineralreich. *Messethemenheft Mineralientage München* 38, 40–53.

Liesegang, R.E. (1915) *Die Achate*, Theodor Steinkopff, Dresden und Leipzig.

Lillie, R.S. (1917) The formation of structures resembling organic growths by means of electrolytic local action in metals, and the general physiological significance and control of this type of action. *Biol. Bull.* 33, 135–186.

Lillie, R.S. and Johnston, E.N. (1919) Precipitation structures simulating organic growth. II. *Biol. Bull.* 36, 225–273.

Little, C.T.S., Herrington, R.J., Haymon, R.M., and Danelian, T. (1999) Early Jurassic hydrothermal vent community from the Franciscan Complex, San Rafael Mountains, California. *Geology* 27, 167–170.

Liu, S.V., Zhou, J., Zhang, C., Cole, D.R., Gajdarziska-Josifovska, M., and Phelps, T.J. (1997) Thermophilic Fe(III)-reducing bacteria from the deep subsurface: the evolutionary implications. *Science* 277, 1106–1109.

Lodders, K. (1998) A survey of shergottite, nakhlite and chassigny meteorites whole rock compositions. *Meteorit. Planet. Sci.* 33, A183–A190.

Madigan, M.T., Martinko, J.M., and Parker, J. (1997) *Biology of Microorganisms*, Prentice Hall, London.

Madsen, E.L. and Bollag, J.M. (1989) Aerobic and anaerobic microbial activity in deep subsurface sediments from the Savannah River Plant. *Geomicrobiol. J.* 7, 93–102.

Markl, G., von Blanckenburg, F., and Wagner, F. (2006) Iron isotope fractionation during hydrothermal ore deposition and alteration. *Geochim. Cosmochim. Acta* 70, 3011–3030.

McKay, D.S., Gibson, E.K., Thomas-Keprta, K.L., Vali, H., Romanek, C.S., Clemett, S.J., Chillier, X.D.F., Maechling, C.R., and Zare, R.N. (1996) Search for past life on Mars: possible relic biogenic activity in martian meteorite ALH84001. *Science* 273, 924–930.

McKinley, J.P., Stevens, T.O., and Westall, F. (2000) Microfossils and paleoenvironments in deep subsurface basalt samples. *Geomicrobiol. J.* 17, 43–54.

Melchiorre, E.B. and Williams, P.A. (2001) Stable isotopic charcterization of the thermal profile and subsurface biological activity during oxidation of the Great Australia Deposit, Cloncurry, Queensland, Australia. *Econ. Geol.* 96, 1685–1693.

Melchiorre, E.B., Williams, P.A., and Bevins, R.E. (2001) A low temperature oxygen isotope thermometer for cerussite, with applications at Broken Hill, New South Wales, Australia. *Geochim. Cosmochim. Acta* 65, 2527–2533.

Melim, L.A., Northup, D.E., Boston, P.J., Queen, J.M., and Allen, C.C. (1999) Evidence for bacterially mediated precipitation of Pool Fingers, Hidden Cave, Guadalupe Mountains, NM. In *American Association of Petroleum Geologists Annual Meeting*, American Association of Petroleum Geologists, Tulsa, OK, A92.

Milliken, K.L. (2001) Endolithic microbial communities in fractures: insights gleaned from mineralized filaments in Cretaceous-age calcite veins in serpentinized peridotites, Iberia abyssal plain [abstract 1010]. In *32nd Lunar and Planetary Science Conference,* Lunar and Planetary Institute, Houston.

Molisch, H. (1910) *Die Eisenbakterien*, Gustav Fischer, Jena.

Motyka, J. and Szurawinski, M. (1989) Growth of speleothems below the karst-water table: considerations on the genesis of sulfide stalactites from the Upper Silesian Zn-Pb ore bodies. *Rocz. Pol. Tow. Geol.* 59, 417–433.

Pedersen, K. (2000) Exploration of deep intraterrestrial microbial life: current perspectives. *FEMS Microbiol. Lett.* 185, 9–16.

Pfeifer, H.R., Oberhänsli, H., and Epprecht, W. (1988) Geochemical evidence for a synsedimentary hydrothermal origin of Jurassic iron-manganese deposits at Gonzen (Sargans, Helvetic Alps, Switzerland). *Mar. Geol.* 84, 257–272.

Popa, R., Kinkle, B.K., and Badescu, A. (2004) Pyrite framboids as biomarkers for iron-sulfur systems. *Geomicrobiol. J.* 21, 193–206.

Pracejus, B. and Halbach, P. (1996) Do marine moulds influence Hg and Si precipitation in the hydrothermal JADE field (Okinawa Trough)? *Chem. Geol.* 130, 87–99.

Rasmussen, B. (2000) Filamentous microfossils in a 3235-million-year-old volcanogenic massive sulphide deposit. *Nature* 405, 676–679.

Razumovsky, G. (1835) Les agates mousseuses. *Bull. Géol. Soc. France* 6, 165–168.

Reitner, J. (2004) Fossile tiefe Biosphäre in Klüften des Triberg Granits (Moosengrund, Schwarzwald). In *Geobiologie. 74. Jahrestagung der Paläonto-logischen Gesellschaft, Göttingen, 02. bis 08. Oktober 2004. Kurzfassungen der Vorträge und Poster,* edited by J. Reitner, M. Reich, and G. Schmidt, Universitätdrucke Göttingen, Göttingen.

Renault, B. (1896) *Flore fossile. Bassin houllier et permien d'Autun et d'Epinac*. Paris.

Reysenbach, A.-L. and Cady, S.L. (2001) Microbiology of ancient and modern hydrothermal systems. *Trends Microbiol.* 9, 79–86.

Robinson, B.W. and Kusakabe, M. (1975) Quantitative preparation of SO_2 for $^{34}S/^{32}S$ analysis from sulphides by combustion with cuprous oxide. *Anal. Chem.* 47, 1179–1181.

Schopf, J.W., Kudryavtsev, A.B., Agresti, D.G., Wdowiak, T.J., and Czaja, A.D. (2002) Laser-Raman imagery of Earth's earliest fossils. *Nature* 416, 73–76.

Schumann, G., Manz, W., Reitner, J., and Lustrino, M. (2004) Ancient fungal life in north Pacific Eocene oceanic crust. *Geomicrobiol. J.* 21, 241–246.

Spilde, M.N., Brearley, A.J., and Papike, J.J. (2001) Mn-oxide minerals from terrestrial cave environments: biomarkers for the search for life on Mars? [abstract 1454] In *32nd Lunar and Planetary Science Conference*, Lunar and Planetary Institute, Houston.

Squyres, S.W., Arvidson, R.E., Bell, J.F., Bruckner, J., Cabrol, N.A., Calvin, W., Carr, M.H., Christensen, P.R., Clark, B.C., Crumpler, L., Des Marais, D.J., D'Huston, C., Economou, T., Farmer, J., Farrand, W., Folkner, W., Golombek, M., Gorevan, S., Grant, J.A., Greeley, R., Grotzinger, J., Haskin, L., Herkenhoff, K.E., Hviid, S., Johnson, J., Klingelhöfer, G., Knoll, A.H., Landis, G., Lemmon, M., Li, R., Madsen, M.B., Malin, M.C., McLennan, S.M., McSween, H.Y., Ming, D.W., Moersch, J., Morris, R.V., Parker, T., Rice, J.W., Jr., Richter, L., Rieder, R., Sims, M., Smith, M., Smith, P., Soderblom, L.A., Sullivan, R., Wänke, H., Wdowiak, T., Wolff, M., and Yen, A. (2004) The Opportunity Rover's Athena science investigation at Meridiani Planum, Mars. *Science* 306, 1698–1703.

Stauffer, R.E. and Thompson, J.M. (1984) Arsenic and antimony in geothermal waters of Yellowstone National Park, Wyoming, USA. *Geochim. Cosmochim. Acta* 48, 2247–2561.

Stein, L.Y. and Nealson, K.H. (1999) Manganese, Metallogenium, and martian microfossils [abstract 6133]. In *Fifth International Conference on Mars*, Lunar and Planetary Institute, Houston.

Stevens, T. (1997) Lithoautotrophy in the subsurface. *FEMS Microbiol. Rev.* 20, 327–337.

Stevens, T.O. and McKinley, J.P. (1995) Lithoautotrophic microbial ecosystems in deep basalt aquifers. *Science* 270, 450–454.

Stubblefield, S.P. and Taylor, T.N. (1988) Recent advances in palaeomycology. *New Phytol.* 108, 3–25.

Taylor, S.R. and McLennan, S.M. (1985) *The Continental Crust: Its Composition and Evolution*, Blackwell, Oxford.

Tazaki, K., Aoki, A., Asada, R., Kishigami, Y., Matsumoto, K., Ohno, M., Sakurayama, K., Shikaura, H., Tawara, K., Ueshima, M., Watanabe, H., and Yamamura, T. (1998) A new world in the science of biomineralization—environmental biomineralization in microbial mats in Japan. *Science Reports of Kanazawa University* XLII(1,2), 1–65.

Trewin, N.H. and Knoll, A.H. (1999) Preservation of Devonian chemotrophic filamentous bacteria in calcite veins. *Palaios* 14, 288–294.

Walczyk, T. and von Blanckenburg, F. (2002) Natural iron isotope variations in human blood. *Science* 295, 2065–2066.

Walsh, M.M. and Lowe, D.R. (1985) Filamentous microfossils from the 3500-myr-old Onverwacht group, Barberton Mountain Land, South Africa. *Nature* 314, 530–532.

Walsh, M.M. and Westall, F. (2003) Archean biofilms preserved in the 3.2–3.6 Ga Swaziland Supergroup, South Africa. In *Fossil and Recent Biofilms: A Natural History of the Life on Earth,* edited by W.E. Krumbein, D.M. Paterson, and G.A. Zavarzin, Kluwer Academic Publishers, Dordrecht, pp. 307–316.

Walter, M.R., Des Marais, D.J., Farmer, J.D., and Hinman, N.W. (1996) Lithofacies and biofacies of Mid-Palaeozoic thermal spring deposits in the Drummond Basin, Queensland, Australia. *Palaios* 11, 497–518.

Walter, M.R., McLoughlin, S., Drinnan, A.N., and Farmer, J.D. (1998) Paleontology of Devonian thermal spring deposits, Drummond Basin, Australia. *Alcheringa* 22, 285–314.

Weiss, B.P., Yung, Y.L., and Nealson, K.H. (2000) Atmospheric energy for subsurface life on Mars? *Proc. Natl. Acad. Sci. U.S.A.* 97, 1395–1399.

Weitschat, W. (1986) Phosphatisierte Ammonoideen aus der Mittleren Trias von Central-Spitzbergen. *Mitt. Geol.-Paläont. Inst. Univ. Hamburg* 61, 249–279.

Welch, S.A., Beard, B.L., Johnson, C.M., and Braterman, P.S., (2003) Kinetic and equilibrium Fe isotope fractionation between aqueous Fe(II) and Fe(III). *Geochim. Cosmochim. Acta* 67, 4231–4250.

Westall, F., Steele, A., Toporski, J., Walsh, M., Allen, C., Guidry, S., McKay, D., Gibson, E., and Chafetz, H. (2000) Polymeric substances and biofilms as biomarkers in terrestrial materials: implications for extraterrestrial samples. *J. Geophys. Res.* 105, 24511–24527.

Westall, F., De Ronde, C.E.J., Southam, G., Grassineau, N., Colas, M., Cockell, C., and Lammer, H. (2006) Implications of a 3.472–3.333 Gyr old subaerial microbial mat from Barberton greenstone belt, South Africa, for the UV environmental conditions on the early Earth. *Philos. Trans. R. Soc. Lond., B, Biol. Sci.* 361, 1857–1875.

Yamaguchi, K.E., Johnson, C.M., Beard, B.L., and Ohmoto, H. (2005) Biogeochemical cycling of iron in the Archean-Paleoproterozoic Earth: constraints from iron isotope variations in sedimentary rocks from the Kaapvaal and Pilbara Cratons. *Chem. Geol.* 218, 135–169.

Zavarzin, G.A. (1981) The genus *Metallogenium*. In *The Prokaryotes,* Vol. 1, edited by M.P. Starr, Springer, New York, pp. 524–528.

Zierenberg, R.A. and Schiffman, P. (1990) Microbial control of silver mineralization at a sea-floor hydrothermal site on the northern Gorda Ridge. *Nature* 348, 155–157.

Address reprint requests to:
Beda A. Hofmann
Natural History Museum Bern
Bernastrasse 15
CH-3005 Bern, Switzerland

E-mail: beda.hofmann@geo.unibe.ch